BNWL-1944
UC-70

Radiation Effects in Solidified High-Level Wastes—Part 1, Stored Energy

January 1976

Prepared for the U.S. Energy Research and Development Administration under Contract E(45-1):1830

Battelle
Pacific Northwest Laboratories

BNWL-1944

DISCLAIMER

NOTICE

PACIFIC NORTHWEST LABORATORY
operated by
BATTELLE
for the
U.S. ENERGY RESEARCH AND DEVELOPMENT ADMINISTRATION
Under Contract E(45-1)-1830

Printed in the United States of America
Available from
National Technical Information Service
U.S. Department of Commerce
5285 Port Royal Road
Springfield, Virginia 22151
Price: Printed Copy $6.00; Microfiche $2.25

ERDA-RL RICHLAND, WA

RADIATION EFFECTS IN SOLIDIFIED HIGH-LEVEL WASTE PART I, STORED ENERGY

by
F. P. Roberts
G. H. Jenks*
C. D. Bopp*

January 1976

* Staff Members of Oak Ridge National Laboratory

Battelle
Pacific Northwest Laboratories
Richland, Washington 99352

THIS PAGE
WAS INTENTIONALLY
LEFT BLANK

CONTENTS

LIST OF FIGURES v

LIST OF TABLES vii

INTRODUCTION 1.1

SUMMARY 2.1

Borosilicate Glass 2.2

Calcine and Al_2O_3 . . . . . 2.3

Hot-Press Compacts and Fused Silica 2.3

COMPOSITION OF HIGH-LEVEL WASTE 3.1

Radioactive Composition 3.1

Chemical Composition 3.1

THEORETICAL CONSIDERATIONS 4.1

Relative Damaging Effects of Different Radiations Formed and Absorbed within Radioactive Wastes. 4.1

Comparisons Between Radiation Damage in Experimental Irradiations and in Radioactive Wastes 4.4

^{244}Cm-Spiked Glass Samples 4.4

Fast Neutron-Irradiated Samples of Synthetic Wastes . . . 4.5

EXPERIMENTAL APPROACH 5.1

Preparation of Specimens 5.1

Irradiation 5.4

Neutron Irradiation 5.4

Preparation of Samples for Irradiation and Calorimetric Measurements 5.7

General Description of Irradiation Assembly 5.7

Recovery of Irradiated Samples 5.9

Gamma-ray Absorption in Samples 5.9

Fast Neutron Flux, Fluence and Energy Spectrum 5.9

Amount of Neutron-Recoil-Damage-Energy in Irradiated Samples and Comparison with Alpha-RN Energy in Actual Wastes. . . 5.11

Alpha Irradiation 5.12

Calorimetry 5.13

Differential Scanning Calorimeter 5.16

Calibration of the DSC 5.18

Calculations of Results 5.18
Accuracy of the DSC Measurements. 5.20
Drop Calorimetry 5.21
Design of the Drop Calorimeter 5.21
Calibration of the Drop Calorimeter 5.21
Accuracy of Drop Calorimeter Measurements 5.23
EXPERIMENTAL RESULTS 6.1
Alpha-Irradiated Specimens 6.1
Stored Energy Release Behavior 6.1
Buildup of Stored Energy with Increasing Alpha Dose. . . . 6.4
The Effect of Storage Temperatures on Stored Energy . . . 6.5
Neutron-Irradiated Specimens 6.8
Presentation of Data 6.8
Discussion of Results with Neutron-Irradiated Specimens . . 6.23
CONCLUSIONS 7.1
Predicted Amounts of Stored Energy and Amounts and Effects of Temperature Excursions in the Event of Stored Energy Release . . 7.1
Comparison of the Effects of Alpha and Neutron Irradiation . . 7.4
REFERENCES 8.1

LIST OF FIGURES

1a	Alpha Dose to Wastes	3.3
1b	Neutron Dose to Wastes	3.3
1c	Beta Dose to Wastes	3.3
2	Neutron Irradiation Assembly	5.8
3	DSC Scans Showing Release of Stored Energy	5.17
4	DSC Sensitivity Factor as a Function of Temperature	5.19
5	Roux-Type Drop Calorimeter	5.22
6	Energy Release Rates of Alpha-Irradiated Specimens	6.2
7	Buildup of Stored Energy with Alpha Dose	6.5
8	Stored-Energy Buildup with Age of Waste	6.6
9	Build-up of Stored Energy with Alpha Dose for Specimens Held at 250°C	6.7
10	Annealing of Stored Energy	6.7
11	ΔT Versus Temperature for Unirradiated SEN-1	6.12
12	ΔT Versus Temperature for Unirradiated SEN-2	6.13
13	ΔT Versus Temperature for Unirradiated SEN-3	6.13
14	ΔT Versus Temperature for Unirradiated SEN-4 and SEN-5	6.14
15	ΔT Versus Temperature for Unirradiated SEN-7	6.14
16	ΔT Versus Temperature for Unirradiated SEN-9	6.15
17	Energy Release Rate Versus Temperature for Neutron-Irradiated SEN-1	6.15
18	Energy Release Rate Versus Temperature for Neutron-Irradiated SEN-2	6.16
19	Energy Release Rate Versus Temperature for Neutron-Irradiated SEN-3	6.16
20	Energy Release Rate Versus Temperature for Neutron-Irradiated SEN-4	6.17

21 Energy Release Rate Versus Temperature for Neutron-Irradiated SEN-5 6.17

22 Energy Release Rate Versus Temperature for Neutron-Irradiated SEN-7 6.17

23 Energy Release Rate Versus Temperature for Neutron-Irradiated SEN-9 6.18

LIST OF TABLES

1	Radioactivity in High-Level Wastes	3.2
2	Typical Materials in High-Level Liquid Waste	3.5
3	Energy Dissipated in Elastic Collisions by Various Nuclear Radiations, and Accumulations of Elastic-Collision-Energies in Radioactive Wastes	4.2
4	Composition of Borosilicate Glass 72-68	5.2
5	Composition of Curium Oxide	5.3
6	Description of Neutron Irradiated Specimens	5.5
7	Calcine Compositions Used in Preparation of Samples for Neutron Irradiation and Stored Energy Measurements	5.6
8	Normalized Fluxes for Energies >0.18 MeV for Experiments in ORR Position A-2	5.10
9	Neutron Fluxes, Exposure Times, and Fluences in ORR Irradiated Samples	5.11
10	Amounts of Neutron-Damage-Energy in Irradiated Samples, and Times to Accumulate Equivalent Amounts of Alpha-RN Energy in Wastes	5.12
11	Enthalpy Change of 12-week Irradiated Specimens upon Heating, and Average Heat Capacity of Irradiated and Unirradiated Specimens After Annealing; Drop Calorimeter	6.9
12	Enthalpy Change of 6-Week Irradiated Specimens upon Heating, and Average Heat Capacity Irradiated and Unirradiated Specimens After Annealing; Drop Calorimeter	6.10
13	Enthalpy Change upon Heating Unirradiated Specimens: Drop Calorimeter	6.11
14	Effect of Irradiation on the Average Heat Capacity of Glass Samples Measured Below the Annealing Temperature, Drop Calorimeter	6.12
15	Enthalpy Changes upon Heating and Ratios of the Values at Different Annealing Temperatures for Neutron-Irradiated Alumina	6.19

16	Enthalpy Changes upon Heating and Ratios of the Values Measured at Different Temperatures for Neutron-Irradiated Fused Silica	6.19
17	Enthalpy Changes Observed upon Heating Samples of Calcine, SEN-2	6.20
18	Enthalpy Changes Observed upon Heating Samples of Calcine on Alumina, SEN-1	6.20
19	Enthalpy Changes Observed upon Heating Samples of Hot Press, SEN-7	6.21
20	Enthalpy Changes Observed upon Heating Samples of Borosilicate Glass, SEN-4	6.21
21	Enthalpy Changes Observed upon Heating Samples of Borosilicate Glass, SEN-5	6.22
22	Average Heat Capacity Observed in Samples of SEN-4 and SEN-5	6.22
23	Maximum Temperature Rises Resulting from Stored Energy Release	7.2
24	Comparison of Stored Energy for Neutron and Alpha Irradiations at Equivalent Damage Energies	7.4

RADIATION EFFECTS IN SOLIDIFIED HIGH-LEVEL WASTE
PART I, STORED ENERGY

F. P. Roberts, G. H. Jenks and C. D. Bopp

1.0 INTRODUCTION

Investigation of radiation-induced stored energy in solidified high-level power reactor waste is part of the ongoing Waste Fixation Program at Battelle, Pacific Northwest Laboratories. One goal of this program is to fully characterize the potential solid forms in which the high-level waste may be incorporated.

Knowledge of the thermal characteristics of the solidified wastes is important in developing containment, transportation, storage, and disposal systems. Of particular concern are the safety-related aspects of these systems. Although stored energy is not generally believed a serious hazard, a full understanding of the amount of energy involved and of the annealing behavior is necessary for a comprehensive safety evaluation. If the quantity of stored energy is large and the release rate high, the temperature rise resulting from a release could be excessive with respect to the effects of high temperatures on the integrity of the waste-container and on the physical and chemical properties of the solid wastes. Also, for very rapid temperature increases the rapid release of mechanical energy accompanying the sudden temperature rise in the wastes might be of concern. The amount of radiation energy which is stored at relatively low waste-temperatures is of particular interest since the wastes will be stored in canisters in water basins for some ten years after reprocessing, and since rapid increases in temperature to effect rapid release of stored energy might occur during removal and/or transport of the canisters to another location. Storage of energy after burial in a repository is also of interest; again from the standpoints of creation of excessively high temperatures and of rapid formation of mechanical energy upon sudden release of the stored energy.

A study was undertaken jointly at Battelle, Pacific Northwest Laboratories, and Oak Ridge National Laboratory to experimentally determine, under various storage conditions, the amounts of stored energy and its release behavior for several different solidified waste forms which are under investigation at PNL. This work is reported in this paper.

Radiation damage resulting in stored energy is expected to be produced mainly by collision processes rather than ionization. In the solidified waste the damage will be induced chiefly by the alpha-recoils from decay of the actinide elements. Thus, this study was designed to simulate the effects of alpha decay. This was done by incorporating alpha emitting ^{244}Cm in synthetic wastes and by neutron irradiation, which is expected to produce damage similar to alpha decay.

The work involving alpha irradiations is on-going. The continuing program will extend the stored energy data to alpha doses equivalent to high-level waste storage periods beyond 10^4y.

2.0 SUMMARY

The buildup and release behavior of radiation-induced stored energy was investigated for several synthetic solidified high-level waste forms with the objectives of evaluating the possibilities of sudden release of the stored energy, and the hazards to the safe handling and containment of the waste which might result from a sudden release. The waste forms included two borosilicate glass formulations, calcine, calcine on Al_2O_3 and a hot press compact of 50% waste oxide-50% quartz. Fused silica and Al_2O_3, without waste oxides, were also investigated. The average heat capacities of some of the materials were also measured to determine whether the radiation damage affected this property.

The materials were irradiated either by internal alpha radiation (by incorporating ^{244}Cm in the solid) or by neutron irradiation in ORR. The irradiations simulated the effects resulting from self-irradiation of the waste for storage periods up to nearly 1000 years for wastes from PWR-UO_2 fuel [equivalent to periods of $\sim$ 10 years for mixed wastes from UO_2 fuel (2/3) and plutonium recycle fuel (1/3)].

The release of the stored energy was measured both by differential scanning calorimetry and by reverse drop calorimetry. The heat capacities of the various materials were obtained by reverse drop calorimetry.

The results of this study showed that the amounts of stored energy which may be accumulated during a period of about 10 years at relatively low storage temperatures following reprocessing are such that only moderate temperature increases ($< 200°C$) in the wastes would occur in the event of sudden release of the stored energy. Extrapolation of the results to longer storage times in a geologic repository together with considerations of available theoretical and experimental information indicated that saturation of energy storage would occur at 50 cal/g or less for each of the waste types; the ΔT corresponding to release of 50 cal/g would be about 250° for most of the waste types. The results of the experimental studies

also showed no apparent way in which a sudden release could occur except as a result of sudden large increases in waste temperature caused by a heat source other than the stored energy.

It was estimated that sudden but transient increases in waste temperatures of up to 200°C following low temperature storage or of up to 250° during long term repository storage would have no serious adverse effects on the waste container or on the physical and chemical properties of the wastes. The maximum linear expansion of wastes which would result from a ΔT of 250°C would be about 0.1%. The steel walls of the waste canister would easily accommodate the stress from this amount of expansion on the diameter and volume of the wastes.

There were no appreciable radiation effects on heat capacities.

2.1 BOROSILICATE GLASS

The buildup of stored energy in the alpha irradiated Cm-spiked borosilicate glass did not reach saturation at irradiation temperatures of 23°C and alpha doses of up to 1.35×10^{18} α/g. However, the increase of stored energy with dose was very small following a dose of about 6×10^{17} α/g (and a stored energy of about 20 cal/g). Linear extrapolation of the experimental relationship between stored energy and dose in the dose range above 6×10^{17} α/g indicated about 35 cal/g stored energy at 10^6 years after burial for the reference 3.3% enriched UO_2 fuel [or at $\sim$ 30,000 years for mixed wastes from UO_2 fuel (2/3) and plutonium recycle fuel 1/3)]. Neutron irradiations produced an apparent saturation at about 20 cal/g at doses equivalent to about 20 years storage of the waste from the UO_2 fuel.

The amount of stored energy accumulated by the borosilicate glass was dependent on the irradiation temperature or storage temperature. Specimens irradiated at 250°C contained only one-third as much stored energy as those irradiated at room temperature. The residual stored energy in irradiated specimens stored at elevated temperature showed a linear decrease with increasing storage temperature. No stored energy was detected in specimens stored at 350°C or higher.

Release rate data showed that the stored energy is released gradually on heating the specimens. The initial release was observed 75° to 100° above the irradiation or storage temperature and was complete at about 600°C. The maximum release rate occurred about 450°C. There were no sharp peaks in the release rate curve.

2.2 CALCINE AND Al_2O_3

Interpretation of the calorimetric measurements of the neutron irradiated calcine and calcine on Al_2O_3 spheres was complicated by irreversible reactions which resulted in enthalpy changes unrelated to stored energy. However, the largest observed net enthalpy change was 25 cal/g at 975°C for the calcine and 15 cal/g at 714°C for the calcine on Al_2O_3. The calcine on Al_2O_3 appeared to have reached saturation at the lower of the two neutron doses.

The Al_2O_3 had not reached saturation at the highest neutron dose, and complete release was not attained at 988°C--the highest calorimeter temperature used. From the data we obtained and that of earlier workers, it was concluded that stored energy may reach at least 50 cal/g at very high doses and at irradiation temperatures of about 100°C.

2.3 HOT-PRESS COMPACTS AND FUSED SILICA

Neutron irradiation of material formed by hot pressing 50-50 mixtures of calcine and quartz showed net enthalpy changes of 30 to 34 cal/g, apparently the saturation value. As with the calcine and calcine on Al_2O_3, irreversible changes occurred on heating. Decomposition caused gas formation at high temperature and limited calorimeter operation to below 840°C.

Measurements on 100% fused silica showed that the stored energy reached saturation during the neutron irradiations and gave a stored energy release of 35 cal/g at 1000°C.

3.0 COMPOSITION OF HIGH-LEVEL WASTE

3.1 RADIOACTIVE COMPOSITION

Radioactivity in the high-level wastes comprises mostly the fission products which decay by beta emission accompanied by gamma photons and the actinide elements with their associated descendents. In general the actinides decay by alpha emissions and to a much smaller extent by spontaneous fission, producing neutrons and fission fragments. Neutrons are also generated by α, n reactions.

The actual spectrum and intensity of the radioactivity in a waste depend on the type of fuel and on its reactor exposure history. The types of fuels of principal concern to waste management today are the light water reactor fuels with and without plutonium recycle (LWR), high temperature gas-cooled reactor fuels (HTGR), and liquid metal fast breeder reactor fuels (LMFBR). Approximate amounts in curies and watts of fission products and actinides (thorium, uranium, neptunium, plutonium and transplutonium elements including daughters) for these four types of fuels are shown in Table 1[1] at cooling times of 10, 100 and 1000 years.

Only the LWR plants are in commercial operation today. Figure 1 shows the alpha, beta and neutron dose accumulation versus time in the wastes from a LWR. The data were calculated using ORIGEN,[2] a versatile code for solving radioactive growth and decay equations. The values are based on a reactor operating at 26.4 MW/MT and a burnup of 33,000 MWd/MT. Curves are presented both for a UO_2 fuel of 3.3% enrichment and for the plutonium fraction of a mixed-oxide plutonium-recycle fuel with 3.5% enrichment. The spent fuel was assumed to be processed 150 days after discharge with a 0.5% uranium and plutonium loss to the high-level waste.

3.2 CHEMICAL COMPOSITION OF WASTES

The reactor fuels are to be processed by chemical dissolution and solvent extraction to recover the uranium and plutonium values. The high-level

TABLE 1. Radioactivity in High-Level Wastes[a]

	LWR-U Amount/MT		LWR-Pu Amount/MT		HTGR Amount/MT		LMFBR Amount/MT	
	Curies	Watts	Curies	Watts	Curies	Watts	Curies	Watts
Fission Products								
10 years	3.2×10^{5}	1.02×10^{3}	2.8×10^{5}	8.7×10^{2}	9.9×10^{5}	3.2×10^{3}	3.2×10^{5}	8.63×10^{2}
100 years	3.5×10^{4}	1.05×10^{2}	3.0×10^{4}	88	1.1×10^{5}	3.3×10^{2}	3.6×10^{4}	1.0×10^{2}
1000 years	17.9	0.012	18.5	0.012	44	0.026	23	0.017
Actinides[b]								
10 years	2.5×10^{3}	71	3.8×10^{4}	1.23×10^{3}	1.1×10^{4}	2.6×10^{2}	1.0×10^{4}	1.7×10^{2}
100 years	4.3×10^{2}	10.2	4.1×10^{3}	1.0×10^{2}	3.9×10^{3}	1.7×10^{2}	6.3×10^{3}	1.2×10^{2}
1000 years	98	3.7	8.2×10^{2}	21.1	3.9×10^{2}	10.0	1.5×10^{3}	32
Reactor Power Level, MW/MT	30		30		65		49	
Fuel Burnup, MWd/MT	33000		33000		94000		37000	
Time of Processing, Days after Discharge	150		150		365		90	

a. Data taken from Reference 1.
b. Assumes 0.5% fuel loss to waste.

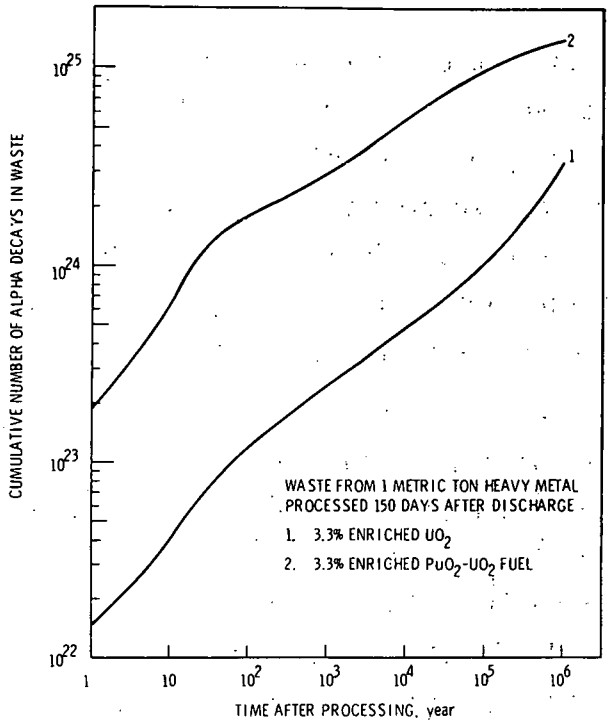

FIGURE 1a. Alpha Dose to Wastes

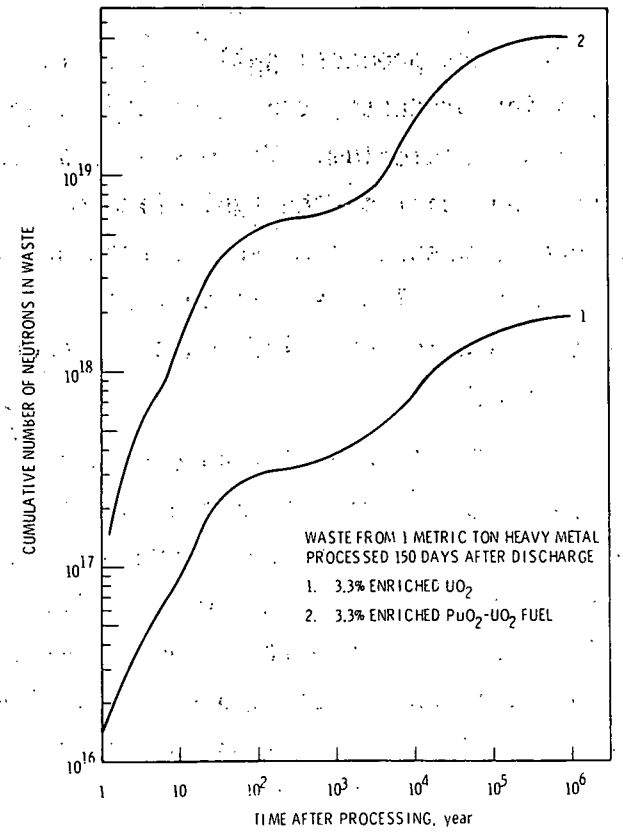

FIGURE 1b. Neutron Dose to Wastes

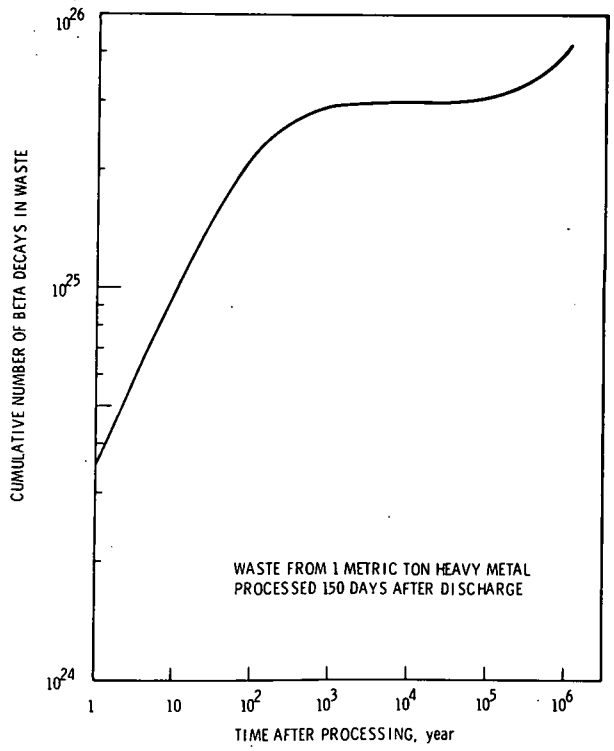

FIGURE 1c. Beta Dose to Wastes

waste from the processing is accumulated as an acidic solution containing the fission products, transplutonium elements and a small fraction of the uranium and plutonium. The wastes also include process chemicals, corrosion products and part of the fuel cladding. Typical expected compositions of the aqueous wastes from various reactor types are shown in Table 2. Actual compositions will depend largely on the recovery and waste handling processes used which will influence the amount of process chemicals and corrosion products.

Solidification of the aqueous wastes may be done by calcination or conversion to monolithic ceramic or glass. Spray, pot and fluidized bed calcination processes have been developed for preparing storable forms. Alternatively, the calcines can be converted to monolithic forms by melting with fluxing agents. The melt-making fluxes include phosphates, borophosphates, silicates, borosilicates and borates. The compositions of the solidified forms evaluated in this study are discussed further in Section 5.1.

TABLE 2. Typical Materials in High-Level Liquid Waste[3]

	Material[b]	Grams/MT from Reactor Type[a] LWR[c]	HTGR[d]	LMFBR[e]
Reprocessing Chemicals	Hydrogen	400	3,800	1,300
	Iron	1,100	1,500	26,200
	Nickel	100	400	3,300
	Chromium	200	300	6,900
	Silicon	--	200	--
	Lithium	--	200	--
	Boron	--	1,000	--
	Molybdenum	--	40	--
	Aluminum	--	6,400	--
	Copper	--	40	--
	Borate	--	--	98,000
	Nitrate	65,800	435,000	244,000
	Phosphate	900	--	--
	Sulfate	--	1,100	--
	Fluoride	--	1,900	--
	Sub-total	68,500	452,000	380,000
Fuel Product Losses[f,g]	Uranium	4,800	250	4,300
	Thorium	--	4,200	--
	Plutonium	40	1,000	500
	Sub-total	4,840	5,450	4,800
Transuranic Elements[g]	Neptunium	480	1,400	260
	Americium	140	30	1,250
	Curium	40	10	50
	Sub-total	660	1,440	1,560
Other Actinides[g]		<0.001	20	<0.001
Total Fission Products[h]		28,800	79,400	33,000
	TOTAL	103,000	538,000	419,000

a. Water content is not shown; all quantities are rounded.
b. Most constituents are present in soluble, ionic form.
c. U-235 enriched PWR, using 378 liters of aqueous waste per metric ton, 33000 MWd/MT exposure. (Integrated reactor power is expressed in megawatt-days [MWd] per unit of fuel in metric tons [MT].)
d. Combined waste from separate reprocessing of "fresh" fuel and fertile particles, using 3,785 liters of aqueous waste per metric ton, 94,200 MWd/MT exposure.
e. Mixed core and blanket, with boron as soluble poison, 10% of cladding dissolved, 1,249 liters per metric ton, 37,100 MWd/MT average exposure.
f. 0.5% product loss to waste.
g. At time of reprocessing.
h. Volatile fission products (tritium, noble gases, iodine and bromine) excluded.

4.0 THEORETICAL CONSIDERATIONS

The principal nuclear radiations formed within high-level wastes are alpha-RNs (recoiling product-nuclei formed in alpha disintegrations), alphas, betas, and gammas. There are also relatively small numbers of fissions and neutrons formed within the wastes.

4.1 RELATIVE DAMAGING EFFECTS OF DIFFERENT RADIATIONS FORMED AND ABSORBED WITHIN RADIOACTIVE WASTES

Nuclear radiations bring about changes, or damage, in waste-type oxides mainly by causing displacement of atoms from their normal lattice positions. With the principal radiations mentioned above, this displacement results mostly from transfer of energy by elastic-collision between the nuclear projectile and atoms in the oxides.*[4] Very energetic, heavy particles such as fission fragments also cause local disorder by intense ionization and/or heat dissipation along the particle track.[5]

The fraction of the energy of a particle which can be dissipated in damage-producing elastic collisions in a given material depends upon the mass and energy of the particle. Some calculated values for the energies thus dissipated by each of the several kinds of radiations in solidified waste are listed in Table 3. Footnotes indicate the methods and assumptions used in the calculations. The assumptions listed under footnote b regarding mechanisms of energy losses above and below E_i** are not completely valid. Some of the energy of the projectile is dissipated in collision processes above E_i and some is dissipated in electronic interactions below E_i.[6] For example, experimental and more accurate theoretical studies have shown that about 25% of the energies of alpha-RNs from Po, Thc, and Thc' in argon are dissipated in forming ion pairs in the gas although the energies of these alpha-RNs are all less than the corresponding values of E_i.[7] The

---

* The amount of energy transferred must exceed some minimum value to produce an isolated displacement stable against spontaneous recombination. This energy E_d depends somewhat on the irradiated material. Generally it is believed to be in the range 25 to 75 eV.

** E_i is the value of E, or energy of the projectile, above which it is assumed that all energy is lost by electronic excitation and below which none is lost by electronic excitation.

fission recoils comprise a special case and require special calculation methods.[8] Despite some possible deficiencies in the calculation methods for the values in Table 3, these upper limit values are quite adequate for comparing relative amounts of damage expected from different radiations within solidified wastes. These comparisons show that the great majority of the initial defect formation will result from alpha-RNs within the wastes.

TABLE 3. Energy Dissipated in Elastic Collisions by Various Nuclear Radiations, and Accumulations of Elastic-Collision-Energies in Radioactive Wastes

Nuclear Particle	Energy Dissipated in Elastic Collisions, KeV	Cumulative Number of Particles in Wastes,[a] Aged 12 and 80 Years (10^{17}/cm^3)		Cumulative Amount of Collision Energy Dissipation in Wastes,[a] Aged 12 and 80 Years (10^{19} KeV/cm^3)	
		12 yr	80 yr	12 yr	80 yr
α-RN (100 KeV)	100[b]	8.1	17.1	8.1	17.1
α(6 MeV)	4 to 8[b,c]	8.1	17.1	0.3 to 0.6	0.7 to 1.4
β(>0.5 MeV; average = 1.5 MeV)	<0.1[d]	3	5	<0.3	<0.5
γ(2 MeV)	<<0.1[e]	<3	<5	<<0.3	<<0.5
Fission recoil	5000[f]	2 x 10^{-5}[g]	4 x 10^{-5}[g]	0.001	0.002

a. For wastes from PWRs with UO_2 fuel; 2 ft^3 of waste per MTHM.[9]
b. Assuming:[4,10] $T < E_i$, all of the kinetic energy of the particle is dissipated in elastic collisions with absorber-atoms. $T > E_i$, all of the kinetic energy of the particle is dissipated in electromagnetic interactions with absorber-electrons. T = kinetic energy of particles. $E_i = 0.001M_2$ MeV where M_2 is the atomic weight of the projectile.
c. Also calculated for waste-type oxides using the method of Kinchin and Pease[8] with E_i as given above.
d. Based on conservatively high estimates for the number of displacements per beta particle together with a value of 50 eV per permanent displacement.[4]
e. Reference 8.
f. Indicated by reported experimental and theoretical values for fission recoils in argon.[7]
g. Reference 11.

The distribution of radiation-induced defects will vary with the kind of radiation. The ranges of heavy particles of a given energy decrease with increasing atomic weight.* Accordingly, the initial damage will be increasingly more localized as the atomic weight of the projectile increases. Beta and gamma radiations will produce more or less isolated defects. As mentioned previously, very energetic, heavy particles may also cause local disorder by intense ionization and/or heat dissipation along the particle track.

Localized deposition of energy by alpha-RNs may or may not produce some damage which would not be present with more even distribution of collision energy. On the one hand, it can be noted that mica and some other naturally occurring silicates which contain small amounts of uranium and thorium can be chemically etched to display the paths of alpha-RNs where they intersect free surfaces.[5] The maximum length of the etched paths of alpha-RNs in mica is about 100 Å, and this length is about one-half the calculated range of the particles.[5] The increased chemical activity in the material along an alpha-RN track presumably results from the disordering of the atoms in this material during passage of the particle.[5] The diameter of the activated material along a track was not established, so that the number of disordered atoms was also not established.** On the other hand, it is known that the structure of zircon is markedly affected by fast neutrons as well as by alpha-RNs from decay of uranium and thorium when these elements are contained in naturally occurring zircon. The changes in structure can be followed by measuring changes in density as well as by X-ray and other types of measurements. The effects of alpha-RNs and neutrons can be compared using data for alpha-RNs and neutrons reported by Holland and Gottfried,[13] and by Crawford and Wittels,[14] respectively. The latter reported that at the highest fluence which they studied--2.8 x 10^{20}/cm^2 > 0.05 MeV fission spectrum--the decrease in density was 4.2%. We estimated that the neutron energy expended in collision processes within the zircon

---

* For example, the reported mean ranges in Al_2O_3 of 72 keV ^{125}Xe and ^{85}Kr are 8.1 and 10.1 μg/cm^2, respectively.[12] At the same energy, the calculated range of ^{234}Th is 5.5 μg/cm^2.[5]

** The etched fission fragment tracts in mica were reported to be about 50 Å in diameter and to have a maximum length of about 20 μ for a pair of recoils.[5] The number of atoms in an etched track of these dimensions is 3 x 10^7.

was 10 to 15 eV per atom.[4] These values are in near agreement with the value of 12 eV per atom of alpha-RN energy which natural zircon has suffered at a 4.2% decrease in density.[4] Others have reported similar conclusions regarding the correspondence between effects of neutrons and alpha-RNs on zircon.[4]

The net rate of defects forming and accumulating during irradiation depends on the recombining and stabilizing (including cluster formation) reactions of the defects as well as on the initial rate of formation. It is then reasonable to expect that the net rate of accumulation of damage will depend upon various exposure variables including:

- Temperature - will influence defect diffusion and reaction rates.
- Type of radiation - as discussed above, will influence the distribution of radiation-induced defects.
- Radiation intensity (dose rate) - the equilibrium between recombination and stabilization reactions may be affected by the rate at which fresh defects are introduced into the solid. Such effects would be most likely when more or less isolated defects are produced by the radiations (beta and gamma radiations). These effects would be much less likely when the fresh defects are formed in clusters (alpha-RN and other heavy particle radiations).
- Dose - the number of accumulated defects within an irradiated material will depend upon dose, and the reactions of freshly formed defects may depend upon the number of defects already present. In general, the total defect density which can be realized at saturation is < 10%.[8]

4.2 COMPARISONS BETWEEN RADIATION DAMAGE IN EXPERIMENTAL IRRADIATIONS AND IN RADIOACTIVE WASTES

4.2.1 ^{244}Cm-Spiked Glass Samples

As shown in Table 3, most of the radiation damage in radioactive wastes will result from alpha-RNs within the wastes. The alpha-RNs from the ^{244}Cm in the spiked samples duplicated these radiations in waste.

The spiked samples differed from actual LWR-UO_2 waste in that dose rates were higher and there were no beta-gamma radiations. On the basis of the arguments in Section 4.1, we do not expect these differences to appreciably affect the relative amounts of stored energy in the samples and wastes at equal alpha-RN doses.* Also in the spiked samples there was no transmutation of elements, which occurs in actual wastes as a result of beta-decay or radioactive elements. However, it can be estimated that the number of transmutations will be small compared to the number of atoms which are disordered if appreciable amounts of radiation energy are stored. For example, the change in elemental species composition in radioactive wastes would be less than 0.1% during the first 100 years following reprocessing, while about 5% of the atoms would be disordered when the stored energy corresponds to 20 cal/g, if it is assumed that a disordered atom has an energy of 1 eV above that of its stable position in the lattice.

4.2.2 Fast Neutron Irradiated Samples of Synthetic Wastes

Fast neutrons undergo elastic collisions with, and transfer energy to, atoms along their paths. The recoil atoms constitute energetic particle radiations within the neutron irradiated material. The recoils will simulate alpha-RN radiations if the elastic collision energy-dissipation per unit path, and the length of path over which this energy is dissipated, are comparable to those of alpha-RNs in the material. These conditions are approximated reasonably well by part of the recoils of the atoms of fission product elements within the wastes. The atomic weights of these elements in the synthetic waste samples fall mostly into two broad groups ranging from 87.5 (Sr) to 112.4 (Cd) in one group and from 127.6 (Te) to 157.3 (Gd) in the other. Roughly 50 atom% of the fission product elements are in each group. The more or less representative values of E_i for these groups are 0.095 and 0.14 MeV, respectively, for the lower and higher atomic weight groups. These compare with alpha-RN energies of about 0.1 MeV. The ranges

---

* Most of the energy of alpha particles is dissipated in the same way that beta and gamma energies are dissipated, i.e., by excitation and ionization of bound electrons. In LWR-Pu wastes, the energy from absorption of alpha particles exceeds that from absorption of betas and gammas. In LWR-U wastes, the alpha absorption energy is less than 10% of the total during the first 100 years following reprocessing. At 1000 years and longer, the alpha energies exceed those of the beta and gammas.[9]

of 0.1 MeV fission product element recoils will be somewhat greater than those of alpha-RNs of the same energy; about 75% and 35% greater, respectively. Accordingly, the density of collision-energy dissipation along the recoil tracks will be about 60% and 75% of that for the alpha-RNs. We assumed that these differences would not appreciably affect the relative amounts of stored energy in the samples and wastes at equal doses of alpha-RN energy and of energy absorbed below E_i from primary recoils of fission product elements formed with energies greater than some minimum energy which is an appreciable fraction of the alpha-RN energy. We arbitrarily set this minimum value at one-fourth of the alpha-RN energy or 0.025 MeV. We compared these absorbed energy quantities in our estimates of the relative damaging effects of a given fluence of fast neutrons to the synthetic samples and of the alpha-RNs within radioactive wastes.

Of course, many displaced atoms would be formed by recoils which are formed with primary energies less than 0.025 MeV in the case of atoms of fission product elements and by recoils of atoms of other, lower atomic weight, elements included in the samples of synthetic wastes. These displacements were neglected in our comparisons between radiation effects in the samples and expected effects in wastes.

The rates of deposition of collision and electron-excitation energy were much higher in the neutron irradiations than those which will prevail in wastes. From information discussed in Sections 4.1 and 4.2.1 we conclude that these differences would not affect the relative amounts of stored energy in the reactor samples and in the wastes.

The synthetic samples were surrounded by 7.2×10^{21} atoms of $^{10}B/cm^2$ during in-pile exposures. Accordingly, any boron contained within the synthetic samples did not undergo any significant amount of absorption of thermal or resonance neutrons. Atoms of other elements within the synthetic samples did undergo some n,γ reactions with resonance energy neutrons. Using information on resonance integral cross sections[15] and on the resonance flux in the ORR core (about 1/10 the unperturbed thermal flux), it can be shown that the number of n,γ reactions was smaller than the 0.1%

of constituent atoms in wastes which would decay by beta-emission during the first 100 years after reprocessing of the wastes.

Summarized below are the equations employed in evaluating the numbers and energies of recoil atoms in the neutron irradiations. These have been previously described,[4] but they are included here for convenient reference.

The maximum energy T_m transferred to an atom from a neutron in an elastic collision is dependent upon the atomic weight of the struck atom M_2 and the neutron energy E_n:

$$T_m = \frac{4M_2}{(M_2 + 1)^2} E_n. \qquad (1)$$

At high M_2,

$$T_m \simeq \frac{4E_n}{M_2}. \qquad (1a)$$

The average energy $\overline{T}$ of the primary recoils between the energy limits

T_1 to T_u is $(T_u \leq T_m)$

$$\overline{T} = 1/2\ (T_u^2 - T_1^2)/(T_u - T_1). \qquad (2)$$

The total energy T_T of the primary recoils (assuming isotropic scattering) in this energy range is

$(T_u \leq T_m)$

$$T_T = \frac{\sigma_n}{2\overline{T}_m} (T_u^2 - T_1^2) \qquad (3)$$

where σ_n is the neutron scattering cross section.

The number of primary recoils N_T between these energy limits is

$(T_u \leq T_m)$

$$N_T = \frac{\sigma_n}{\overline{T}_m} (T_u - T_1). \qquad (4)$$

In evaluating Equation (3) for a spectrum of neutron energies, we have Equations (5-7) for different ranges of neutron and primary recoil energies relative to E_i.

$T_m \leq E_i$

$$T_T' = \frac{\sigma_n}{2T_m} (E_i^2 - T_1^2) \tag{5}$$

$T_m > E_i$ and $T \leq E_i$

$$T_T'' = \frac{\sigma_n}{2T_m} (E_i^2 - T_1^2) \tag{6}$$

$T_m > E_i$ and $T > E_i$

$$T_T''' = \frac{\sigma_n}{T_m} (T_m - E_i)(E_i). \tag{7}$$

Combining Equations (5-7) and substituting for E_i ($E_i = 0.001\ M_2$ MeV, see Table 3) and T_m from Equation (1a).

$$T_T = \sigma_n \left[\frac{2E_n}{M_2} - \frac{T_1^2 M_2}{8E_n} \right] + \sigma_n \left[10^{-3} M_2 - \frac{10^{-6} M_2^3}{8E_n} - \frac{M_2 T_1^2}{8E_n} \right] \tag{8}$$

$$\frac{T_1 M_2}{4} \leq E_n \leq \frac{10^{-3} M_2^2}{4} \qquad E_n \leq \frac{10^{-3} M_2^2}{4}$$

As stated above, we set T_1 equal to 0.025 MeV in our estimates of the relative damaging effects of fast neutrons and of alpha-RNs.

5.0 EXPERIMENTAL APPROACH

The potential solidified waste forms included in this study were:

- two borosilicate glass compositions,
- a calcine prepared by direct drying and denitration of synthetic aqueous waste,
- alumina coated with calcine which simulated the product of the fluidized bed calcination process,
- a compact formed by hot pressing equal amounts of calcine and silica.

One of the borosilicate glasses, Melt 72-68, was selected for detailed study of the buildup of stored energy versus radiation dose and the effects of temperatures on the buildup of stored energy. Specimens of this material were internally irradiated with alpha particles by incorporating ^{244}Cm in the melts.

Specimens of all materials were irradiated in the Oak Ridge Research Reactor for 6 weeks and 12 weeks to obtain two neutron doses. Alumina and quartz without waste oxides were also irradiated in order to determine their contribution to the stored energy in the calcine-on-alumina and the hot-press compact.

The stored energy release was measured both by differential scanning calorimetry and drop calorimetry. Heat capacities before and after irradiation were measured by drop calorimetry. The stored energy release rates and the thermal behaviors before and after irradiation were studied by differential scanning calorimetry.

The preparation of the materials, irradiation and calorimetry are described in this section.

5.1 PREPARATION OF SPECIMENS

The specimens for alpha irradiation were made up to correspond to Melt 72-68, a zinc borosilicate glass incorporating about 25 wt% waste oxides.

Table 4 gives the exact composition of the glass. The glass was prepared in 10-g batches by intimately mixing PW-4b-4 calcine, 73-1 frit, Cm_2O_3 and RuO_2 in the proper ratios. (The ruthenium was added here rather than in the preparation of the calcine to minimize losses due to volatilization of RuO_4.)

The curium used in the specimens was obtained from ORNL as purified curium sesquioxide with the composition given in Table 5.

TABLE 4. Composition of Borosilicate Glass 72-68

Constituent	wt%	Constituent	wt%
S_iO_2	28.21	Ag_2O	0.05
B_2O_3	11.51	CdO	0.06
ZnO	22.04	TeO_2	0.42
Na_2O	4.19	Cs_2O	1.68
K_2O	4.19	La_2O_3	1.87
CaO	1.53	CeO_2	3.75
MgO	1.53	Pr_6O_{11}	0.37
SrO	2.15	Nd_2O_3	1.34
BaO	2.44	Sm_2O_3	0.23
Rb_2O	0.21	Eu_2O_3	0.08
Y_2O_3	0.02	Gd_2O_3	0.16
ZrO_2	2.88	Fe_2O_3	0.88
MoO_3	3.71	Cr_2O_3	0.20
RuO_2	1.73	NiO	0.08
Rh_2O_3	0.28	PO_4^{-3}	0.39
PdO	0.86	Cm_2O_3	1.0

TABLE 5. Composition of Curium Oxide

Component	Concentration, wt%	Alpha Activity, α/min/g
$^{244}Cm_2O_3$	82.1	1.34×10^{14}
$^{245}Cm_2O_3$	0.8	2.9×10^{9}
$^{246}Cm_2O_3$	4.3	2.7×10^{10}
$^{247}Cm_2O_3$	0.1	1.8×10^{5}
$^{240}PuO_2$	11.2	5.0×10^{10}
$^{243}Am_2O_3$	1.2	4.5×10^{9}
Fe_2O_3	0.2	--

The amount of curium oxide added was nominally 1.0 wt%, but varied from specimen to specimen. The actual specific alpha activities in the specimens ranged from 1.2 to 2.2 x 10^{12} α/min/g of glass. This high activity allowed the simulation of several hundred years storage in about 1 year.

Melting was done in an electric furnace in an air atmosphere at 1200°C in a platinum crucible. The melt was held at temperature 3 hr with occasional stirring. The test specimens were formed by pouring the melt onto a stainless steel plate held at 250°C. This resulted in buttons about 3 cm diam and 0.6 cm thick. The buttons were then annealed by heating to 400°C for 2 hr and then were slowly cooled to room temperature.

The buttons were pulverized to a particle size of about 400 μm and placed in controlled temperature storage to allow the alpha dose to build up. Specimen A-27 was divided immediately after annealing. Part was placed in an electric furnace maintained at 250 ± 10°C, and the rest was stored at the ambient temperature of the glove box.* The remainder of the specimens were stored at ambient temperature.

* The ambient temperature of the glove box was controlled with the aid of refrigerated air conditioning always in the range of 19 to 25°C.

Elevated temperature storage conditions were also simulated by placing samples of specimen A-3 in an electric furnace at various temperatures from 100°C to 350°C. The samples were held at the desired temperature 4 weeks, and the stored energy release was determined each week. There was no significant difference in the quantity of energy release after the first week. The value obtained at 250°C by this method agreed with that obtained with specimen A-27, which was always held at 250°C. Thus it was decided that this approach provided a satisfactory estimate of the stored energy as a function of storage temperature.

The anticipated storage conditions of real high-level wastes may result in devitrification of the glass forms. Two of the specimens, A-4 and A-5 were, therefore, treated to induce devitrification, permitting an evaluation of this effect on stored energy buildup. The devitrification was done by holding the buttons at 700°C for 7 days and then slowly cooling to room temperature. These specimens were stored at the ambient glove box temperature, and their stored energy was measured.

In addition to the curium-containing specimens, four other types of material as well as specimens of melt 72-68 were prepared for neutron irradiation in the ORNL reactor. These represented other potential waste forms. Pure quartz and Al_2O_3 were also included in this group. The composition of these materials are shown in Tables 6 and 7.

5.2 IRRADIATION

5.2.1 Neutron Irradiation

In these experiments, four samples of each of the five different synthetic waste compositions and of the alumina and fused silica were exposed to fast neutrons in the A-2 core position in the Oak Ridge Research Reactor (ORR). The sample temperature during irradiation was maintained near 100°C The irradiated samples were later recovered and analyzed for stored energy by the Roux-type drop calorimeter and by the differential scanning calorimeter (see Section 5.3). Two different sets of radiation exposures (6 and 12 weeks) and calorimetric measurements were made.

TABLE 6. Description of Neutron Irradiated Specimens

Identification Number	Description	Composition
SEN-1	Fluidized bed calcine, prepared by an in-bed combustion technique at 500°C, using a starting bed of Al_2O_3 particles.[16]	80-mesh alumina particles[a] (65.3 wt%) coated with Type 2 PW-4b calcine[b] (34.7 wt%).
SEN-2	Calcine prepared by boiling to dryness in stainless steel basket, heating 2 hr at 500°C, and grinding to -20 mesh.	Type 1 PW-4b[b]
SEN-3	Al_2O_3	80-mesh alumina particles[a]
SEN-4	Simulated HLW glass, melted 3 hr at 950°C and cooled at about 100°C/hr.	22.4 SiO_2, 25.2 B_2O_3, 3.5 Na_2O, 3.5 K_2O, 10.6 ZnO, 1.2 CaO, 1.2 MgO, 1.2 SrO, 1.2 BaO, 30 PW-4m waste oxide.
SEN-5[c]	Simulated HLW glass melted 3 hr at 1150°C and cooled at about 100°C/hr.	27.8 SiO_2, 11.3 B_2O_3, 4.1 Na_2O, 4.1 K_2O, 21.7 ZnO, 1.5 CaO, 1.5 MgO, 1.5 SrO, 1.5 BaO, 25 Type 1 PW-4b[b] waste oxide.
SEN-7	Hot pressed composite of quartz and laboratory-prepared calcine, hot pressed for 10 min at 2500 psi and 1000°C.	50 wt% finely divided quartz sand, 50 wt% PW-4m calcine.[b]
SEN-9	Fused Silica	Standard quartz tubing, no analyses of impurities.

a. Norton 38A80, Norton Co., Worcester, MA.
b. Waste compositions are given in Table 7.
c. Melt 72-68, which is identical to the alpha-irradiated specimens except that it contains no Cm_2O_3.

TABLE 7. Calcine Compositions Used in Preparation of Samples for Neutron Irradiation and Stored Energy Measurements

	Weight Percent		
	PW-4b		
	Type 1	Type 2	Pw-4m
Na_2O	--	--	8.29
Fe_2O_3	3.93	9.53	8.21
Cr_2O_3	0.90	1.00	0.71
NiO	0.36	3.02	2.95
P_2O_5	1.74	1.94	--
SiO_2	--	--	0.47
MoO_3	16.59	18.45	18.12
SrO	2.76	3.07	2.88
BaO	4.08	4.53	4.92
Cs_2O	7.49	--	--
K_2O	0.46	3.30	3.40
RE_2O_3*	33.62	37.37	35.15
ZrO_2	12.86	14.30	13.77
RuO_2	7.73	--	--
Co_3O_4	--	0.88	0.84
Rh_2O_3	1.25	--	--
PdO	3.86	--	--
TeO_2	1.89	2.10	--
Ag_2O	0.23	0.25	--
CdO	0.26	0.28	--
CuO	--	--	0.26

* rare earth oxide

5.2.1.1 Preparation of Samples for Irradiation and Calorimetric Measurements

Samples of synthetic wastes and of alumina and fused silica were prepared and/or selected at PNL. These were ground to pass through 40 mesh. The alumina and calcine-coated alumina, supplied in the form of fine particles, required no grinding.

Each sample was prepared for irradiation by hermetically sealing the oxide sample material within a platinum capsule (188 mil OD, 4 mil wall, 0.5 in. long, dished heads, see Figure 2). Prior to final sealing, the capsule was evacuated through an attached capillary (10 mil ID) and simultaneously heated to about 150°C for 5 hr. The capsule was backfilled with 90% He-10% O_2 at 0.5 atm, and the capillary then sealed off. The sample remained in the capsule throughout irradiation and drop calorimetric measurement.* Care was taken in welding to assure that the sample temperature did not exceed about 150°C. To this end, the capsule was held in a copper chill-block when the second head was welded to the body containing the sample.

5.2.1.2 General Description of Irradiation Assembly

The specimen-holder portion of the irradiation assembly is shown in Figure 2. The upper portion of the assembly, not shown, contained a gas reservoir (1 liter volume) into which the helium from $^{10}B,n\alpha,^{7}Li$ reactions could accumulate. The assembly was out-gassed and backfilled with 2 psi of helium before the final weld-seal was made.

The adapter fitted within an aluminum core-experiment piece. Reactor coolant-moderator water flowed down around the assembly and through the 1/16-in. channel between the adapter and the holder. The water within the channel (51°C) carried heat away from the experimental assembly. A careful analysis showed that the temperature of the oxide of maximum bulk density within the platinum capsules would not exceed 110°C at the center and 86°C at the inner walls of a capsule. Other samples with less bulk densities had

* One sample of each irradiated material was measured for stored energy release below 600°C using the differential scanning calorimeter. The sample was removed from the capsule for these measurements.

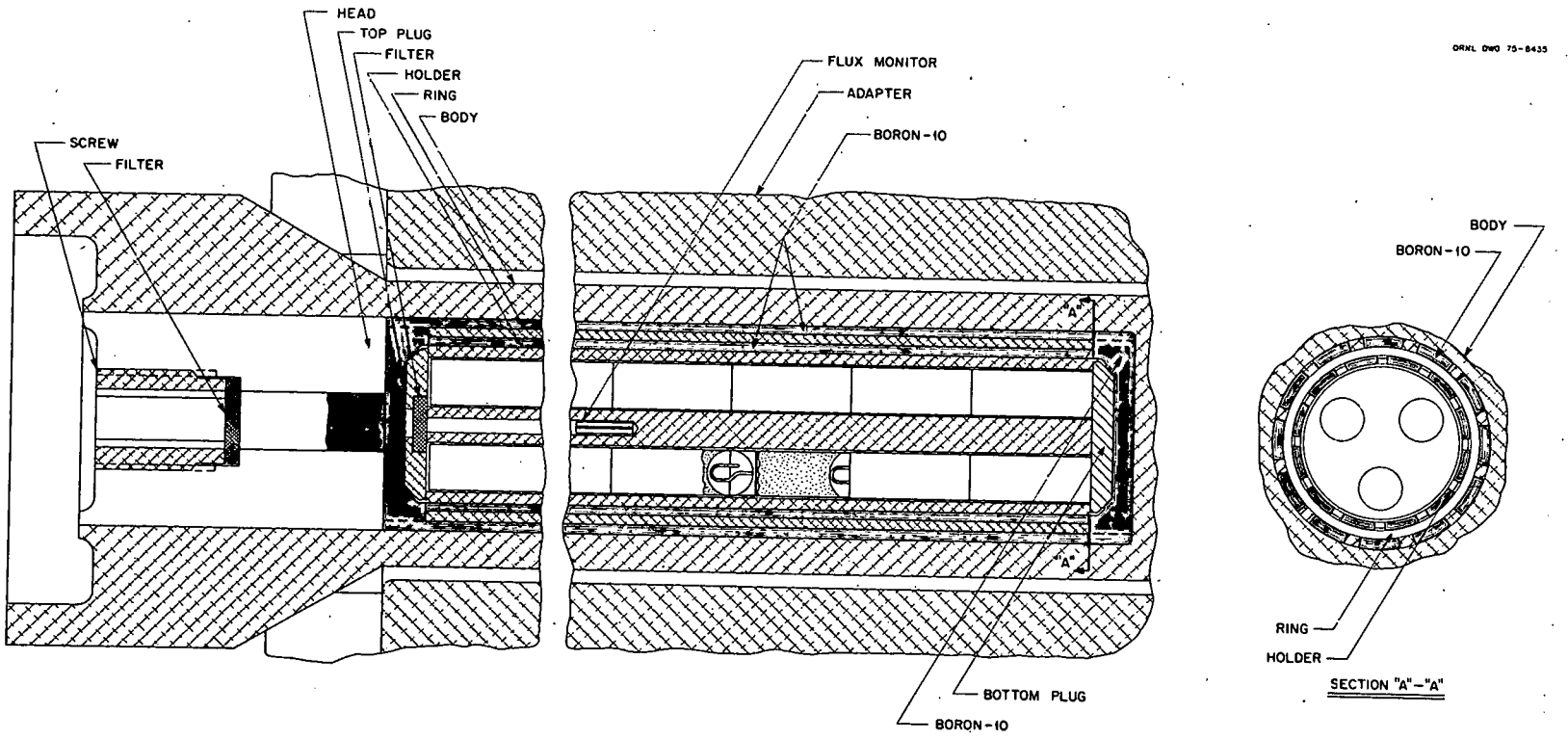

FIGURE 2. Neutron Irradiation Assembly

lower temperatures. For example, SEN-7, for which the bulk density was 1.7, had a calculated temperature ≤102°C at the center and ≤85°C at the inner wall of a capsule.*

The boron metal powder surrounding the specimen holder was 92% boron-10. The loading and enrichment were such that there were 7.2×10^{21} atoms of ^{10}B per cm^2.

5.2.1.3 Recovery of Irradiated Samples

The irradiated capsules were removed from the assemblies by hot-cell operations. Each sample was rinsed, first in water and then in alcohol. It was then placed in a clean brass tube, 1/4 in. ID, 4 in. long, one sample per tube. The samples were transferred to the calorimeter in these tubes.

5.2.1.4 Gamma-ray Absorption in Samples

Information available from reactor operations showed that the rates of absorption of gamma-ray and fast neutron energy in the samples were about 2.5 W/g.

5.2.1.5 Fast Neutron Flux, Fluence and Energy Spectrum

The fast neutron fluxes and energy spectra in the exposures were evaluated by Kerr and Allen[17,18] of ORNL using:

- 123-group neutron energy spectra for several ORR compositions obtained by calculations using one-dimensional models of the ORR, XSDRN-code.
- Three-dimensional map of seven group neutron fluxes obtained by calculations using the relevant core compositions: VENTURE code.
- Results obtained for the number of $^{54}Fe \rightarrow {}^{54}Mn$ reactions in the iron flux monitors which were included in our irradiation assemblies.

The neutron energy spectra for energies >0.18 MeV, which were considered most appropriate for our experimental assembly, the core loading and the flux monitor results, are reported in Table 8 as normalized group fluxes. The results of the flux evaluations are listed in Table 9 together with information on exposure times and neutron fluences.

* Measured bulk densities were: SEN-1, 2.33; SEN-2, 1.51; SEN-3, 1.94; SEN-4, 1.68; SEN-5, 1.73; SEN-7, 1.70; SEN-9, 1.15.

TABLE 8. Normalized Fluxes for Energies >0.18 MeV for Experiments in ORR Position A-2

Energy Group Number	Upper Energy, MeV	Normalized Group Fluxes % Neutrons/cm^2 • sec	
		6 Weeks Irradiation	12 Weeks Irradiation
1	14.92	0.0041	0.0044
2	13.50	0.0107	0.0112
3	12.21	0.0227	0.0238
4	11.05	0.0450	0.0477
5	10.00	0.0818	0.0868
6	9.05	0.134	0.145
7	8.19	0.201	0.222
8	7.41	0.314	0.340
9	6.70	0.448	0.486
10	6.07	0.592	0.649
11	5.49	0.775	0.851
12	4.97	0.959	1.06
13	4.49	1.19	1.30
14	4.07	1.29	1.43
15	3.68	1.35	1.56
16	3.33	1.34	1.63
17	3.01	1.20	1.56
18	2.73	1.99	2.34
19	2.47	3.01	3.21
20	2.23	3.41	3.40
21	2.02	4.08	4.01
22	1.83	4.50	4.30
23	1.65	4.61	4.41
24	1.50	4.46	4.27
25	1.35	4.00	3.87
26	1.22	3.70	3.61
27	1.11	3.49	3.44
28	1.00	3.57	3.51
29	0.907	3.68	3.62
30	0.821	3.38	3.37
31	0.743	3.41	3.42
32	0.672	2.20	2.27
33	0.608	2.85	2.93
34	0.550	3.28	3.31
35	0.498	3.38	3.37
36	0.450	3.33	3.33
37	0.468	3.30	3.22
38	0.364	3.17	3.06
39	0.334	3.09	2.46
40	0.302	2.98	2.84
41	0.273	2.90	2.75
42	0.247	2.80	2.63
43	0.224	2.72	2.53
44	0.202	2.65	2.47
45	0.183		

TABLE 9. Neutron Fluxes, Exposure Times, and Fluences in ORR Irradiated Samples[a]

	6 Week Irradiation	12 Week Irradiation
Flux at full reactor power, $n/cm^2/sec$ >0.18 MeV	0.81×10^{14}	1.03×10^{14}
Reactor energy during irradiation, MW-hr	29,094	56,266
Equivalent exposure time at full reactor power, sec	3.49×10^{6}	6.27×10^{6}
Fluence during irradiation, >0.18 MeV	2.90×10^{20}	6.96×10^{20}
Fluence during irradiation, >1.0 MeV	1.45×10^{20}[b]	3.48×10^{20}[b]

a. Listed values refer to specimens located near the top of the assemblies. The fluxes at specimens near the bottom were 15 to 20% higher. The fluxes at the other locations were intermediate.
b. Using the energy spectra listed in Table 8.

5.2.1.6 Amount of Neutron-Recoil-Damage-Energy in Irradiated Samples and Comparison with Alpha-RN Energy in Actual Wastes

The amounts of energy of those primary recoils of fission product elements which were formed and absorbed at energies >0.025 MeV and $<E_i$, respectively, were calculated using: 1) Equation (8) of Section 4, 2) an assumed value of three barns for σ_s, 3) available information on the percentages of fission product elements in each sample, 4) values listed in Table 8 for the neutron energy spectra, and 5) values listed in Table 9 for the neutron fluences. The calculation results are listed in Table 10. Values are also listed for the times after reprocessing of LWR-UO_2 wastes in which an equivalent amount of alpha-RN energy would accumulate in the wastes.

TABLE 10. Amounts of Neutron-Damage-Energy in Irradiated Samples, and Times to Accumulate Equivalent Amounts of Alpha-RN Energy in Wastes

Sample Number	Irradiation, Weeks	Neutron-Recoil-Damage-Energy,(a) 10^{22} eV/g	Time After Solidification Processing to Accumulate Equivalent Alpha-RN Energy in Wastes,(b) Years
SEN-1	6	1.5	6
	12	4.0	29
SEN-2	6	4.3	58
	12	11.1	>300
SEN-4	6	1.4	4
	12	3.6	23
SEN-5	6	1.3	3.5
	12	3.3	20
SEN-7	6	2.1	9.5
	12	5.6	66

a. See text.
b. For LWR-UO_2 wastes reprocessed and solidified at 150 days after discharge, and with waste volume of 2 ft^3 per MTHM. With mixed LWR-UO_2 (2/3) and LWR-PuO_2 (1/3) waste, the alpha-RN energy of 11.5 x 10^{22} ev/g is accumulated in a period of about 10 years following reprocessing.
c. Within the calcine portion of the composite sample.

5.2.2 Alpha Irradiation

The alpha doses of the curium-containing specimens were calculated from the known amount of Cm_2O_3 added to each specimen and the time elapsed since the specimen was annealed. The ^{244}Cm content of the Cm_2O_3 was estimated from the ORNL analyses given in Section 5.1 and the alpha emission rate based on a half-life of 18 years for ^{244}Cm.

Since the range of alpha-RNs is in the order of 100 Å, as discussed in Section 4, the radiation damage to the glass is quite sensitive to the distribution of the ^{244}Cm in the glass matrix. Agglomeration of the ^{244}Cm in the specimen will result in damage only within the region of the agglomerates. Autoradiographs of the specimens were prepared to verify uniform distribution of the ^{244}Cm. These showed no macro-concentrations of curium but, of course, could not assure the absence of concentrations on a microscale.

5.3 CALORIMETRY

Two different calorimetric techniques were used to measure the stored energy release of the irradiated specimens: transposed-temperature* drop calorimetry (DC) and differential scanning calorimetry (DSC).

In the drop calorimetry, the heat release (or absorption) upon heating a sample to a given temperature was evaluated from two successive measurements of the heat required to raise the temperature of the sample from an initial temperature, T_i, to the given higher temperature, T_h, maintained within the DC. It was assumed (and verified experimentally) that annealing of the sample material and other processes which were activated at the given high temperature and which released (or absorbed) heat were essentially complete during the first measurement. It can then be shown that the difference between the results of the successive DC measurements corresponds to the difference between the enthalpies (ΔH) at the initial temperature (about 125°C) of the annealed and unannealed samples.[19] Various calorimeter temperatures were used up to the maximum operating temperature of about 1000°C.

The differential scanning calorimetry was conducted using a commercially available two-pan instrument in which samples were heated at a constant and reproducible rate from room temperature to the maximum operating temperature, 600°C. The rate of heat release was evaluated from two or three successive measurements of the difference between the temperatures of the sample and that of an inert material in the second pan. The total heat released within a given temperature range was evaluated from the rate-temperature data for that range.

DC and DSC measurements were made on unirradiated as well as on irradiated samples of the same material. This permitted thermal effects, unrelated to radiation effects, that might occur during heating to be taken into account.

As stated above, the results of the DC measurements yielded data for the difference between the enthalpies, at the initial temperature (125°C),

---

* This differs from the usual calorimeter in that the sample is dropped into a receiver that is at a high temperature.

of the annealed and unannealed sample. The changes in states (annealing) of sample materials which bring about changes in enthalpy actually occur at temperatures greater than the initial temperature T_i. The value of ΔH at a higher temperature T_a is the same as that at T_i unless the irradiation and/or heating causes changes in the average heat capacity in the temperature range T_i to T_a. Accordingly, information on heat capacities was of interest. The heat absorption in the second (and subsequent) DC measurement on a sample is a measure of the average heat capacity of the annealed material in the temperature range T_i to T_h, and we evaluated this quantity from the DC data. Heat capacities prior to annealing of radiation damage were evaluated from the results of special DC measurements in the temperature range 75 to 195°C (i.e., $T_i = 75°$ and $T_h = 195°$). The relationships described above are expressed symbolically as follows:

$$\Delta H(T_i) = H_1(T_i) - H_2(T_i) \tag{9}$$

This equation represents the difference between the enthalpies at T_i of the irradiated sample before and after heating from the initial temperature T_i to the DC temperature. The before and after states are represented by sub-one and sub-two, respectively. $\Delta H(T_i)$ is the quantity evaluated in the DC measurement of an irradiated sample.

$$\Delta H'(T_i) = H_1'(T_i) - H_2'(T_i) \tag{10}$$

Equation (10) represents the difference between the enthalpies at T_i of the unirradiated initial material before and after heating from the initial temperature T_i to the DC temperature. $\Delta H'(T_i)$ is the quantity evaluated in the DC measurement of an unirradiated sample.

All of the enthalpies at T_a can be related to those at T_i through heat capacity functions as follows:

$$H_1(T_a) = H_1(T_i) + \int_{T_i}^{T_a} C_1 dT \tag{11}$$

$$H_2(T_a) = H_2(T_i) + \int_{T_i}^{T_a} C_2 dT \tag{12}$$

and subtracting Equation (12) from Equation (11) we have

$$\Delta H(T_a) = \Delta H(T_i) + \int_{T_i}^{T_a} C_1 dT - \int_{T_i}^{T_a} C_2 dT. \tag{13}$$

Similarly

$$H_1'(T_a) = H_1'(T_i) + \int_{T_i}^{T_a} C_1' dT \tag{14}$$

$$H_2'(T_a) = H_2'(T_i) + \int_{T_i}^{T_a} C_2' dT \tag{15}$$

and

$$\Delta H(T_a) = \Delta H'(T_i) + \int_{T_i}^{T_a} C_1' dT - \int_{T_i}^{T_a} C_2' dT \tag{16}$$

where C_1 represents the average heat capacity between T_i and T_a before annealing; and C_2 is the after annealing. The prime refers to the unirradiated sample.

Appropriate combination of the above equations yields

$$[\Delta H(T_a) - \Delta H'(T_a)] = [\Delta H(T_i) - H'(T_i)] + \int_{T_i}^{T_a} C_1 dT - \int_{T_i}^{T_a} C_1' dT$$

$$- \left[\int_{T_i}^{T_a} C_2 dT - \int_{T_i}^{T_a} C_2' dT \right]. \tag{17}$$

However, in most cases it can be shown that the terms involving the heat capacity approximately cancel since the heat capacity usually does not change significantly on annealing. The exceptional cases are discussed in Section 6.

The DSC, unlike the DC, provides a continuous measurement of the stored energy release as a function of temperature and permits observation of features in the release such as the temperature at which the release starts and ends and peaks in the release curve. Complete interpretations of the results of the DSC measurements depend on information, experimental or assumed, regarding the relative heat capacity of a sample material before and after the first heating in the DSC.

The alpha-irradiated specimens were measured exclusively by DSC at PNL. The neutron-irradiated specimens were measured both by DC and DSC. The DSC measurements of the latter specimens were used to substantiate the validity of the DSC technique and to determine the relationships between energy release and temperature during heating.

5.3.1 Differential Scanning Calorimeter

A DuPont Model 990 Thermoanalyzer with a plug-in type DSC cell was used for measuring the stored energy release. The DSC cell was installed inside a glove box with the temperature programmer and recorder outside. No modifications to the instrument was required for use in the glove box. (For a description of this system see DuPont product bulletins available from Instrument Products Division, E. I. DuPont deNemours, Wilmington, DE.)

Samples were prepared for the energy release measurements by weighing 25 to 60 mg of the powdered specimens in small aluminum pans provided by the instrument manufacturer. In the early measurements the irradiated samples were balanced with an equal mass of nonirradiated material of identical composition (except for curium in the case of alpha-irradiated specimens). Later it was found that no significant differences in the observed stored energy resulted if an empty pan was substituted for the reference sample and the reference material was not used from then on.

The calorimetric measurements were made by heating the sample at a constant reproducible rate and recording the differential temperature ΔT (between the sample and the reference thermocouple) and the sample temperature T. The furnace was then allowed to cool and the heating cycle was repeated at least two times. A typical record of a ΔT-T plot is shown in Figure 3.

The heating rate was 20°C/min. Operating at lower rates reduced the sensitivity of the DSC and increased the amount of baseline drift resulting in unsatisfactory measurements. This relatively fast heating rate undoubtedly reduced the capability for resolving peaks in the stored energy release spectra and may have introduced a minor error due to incomplete release during the first heating cycle. This error, if it existed, appears to be small because differences between the second and third heating cycles were small.

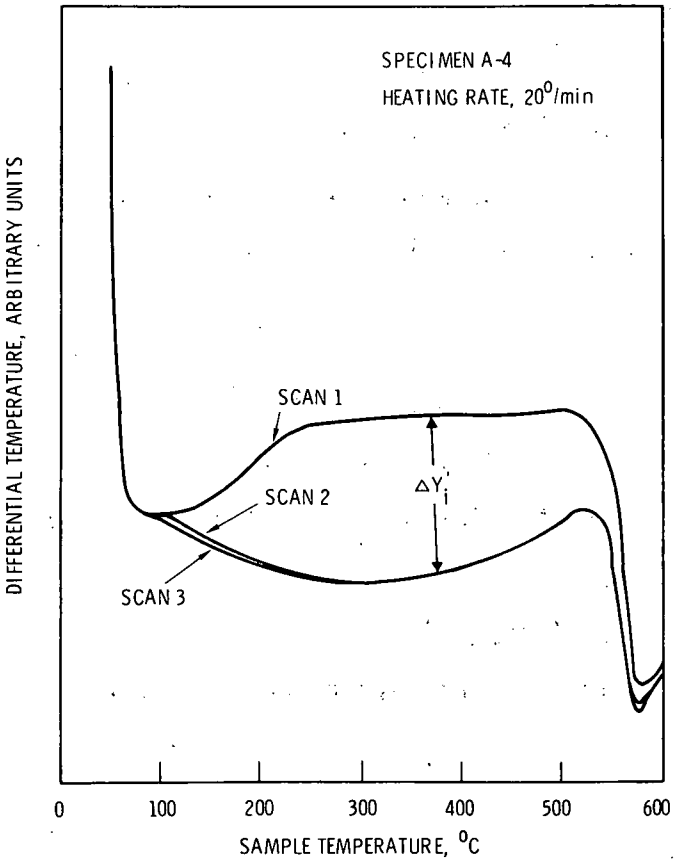

FIGURE 3. DSC Scans Showing Release of Stored Energy

5.3.1.1 Calibration of the DSC

The DSC system was calibrated with a known mass of synthetic sapphire (Al_2O_3) with known heat capacity values from the National Bureau of Standards. The sapphire standard was placed in the calorimeter and heated at the rate for which the system was to be calibrated, and ΔT and T were recorded. A second heating cycle was made with the standard removed. The difference between the ΔT's from the two cycles is dependent on the heat capacity of the standard. A DSC sensitivity factor was calculated from the observed ΔT values and the known values of the heat capacity using

$$F = \frac{C \quad Rm}{\Delta Y} \tag{18}$$

where

C is the heat capacity of the standard at the temperature of interest in cal $\cdot$ $^{\circ}C^{-1} \cdot g^{-1}$

R is the heating rate in $^{\circ}C \cdot sec^{-1}$

m is the mass of the standard in g and

ΔY is the difference in ΔT between the cycle with the standard in place and the cycle without, in arbitrary units (usually inches).

The DSC sensitivity factor varies nonlinearly with temperature as shown in the typical calibration curve given in Figure 4.

The calibration was repeated each week throughout the investigation. The relative standard deviation of the sensitivity factor was 1.9% at 200°C and 2.4% at 500°C.

5.2.1.2 Calculations of Results

The stored energy release rates were calculated from the ΔT-T data and the DSC sensitivity factors by:

$$\frac{dH}{dT} = \frac{\Delta Y_i F}{Rm} \tag{19}$$

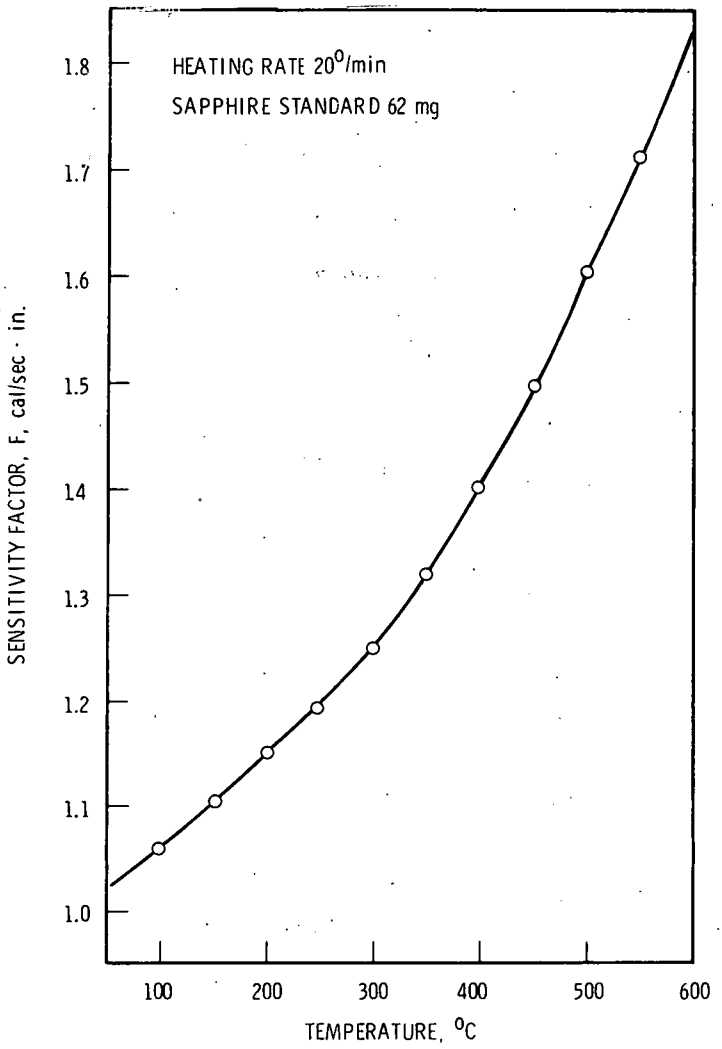

FIGURE 4. DSC Sensitivity Factor as a Function of Temperature

where ΔY_i is the difference between ΔT from the first heating cycle and the average ΔT of subsequent cycles at the temperature of interest, in arbitrary units (inches).

The total energy release was determined by plotting $\frac{dH}{dT}$ versus T and estimating the area under the curve by mechanical integration.

Alternatively the total energy release can be obtained directly from the recorder plots of ΔT versus T. In this case, the area between the first scan and subsequent scans is estimated. The integration must be performed over relatively short temperature intervals because of the nonlinearity of the sensitivity factor F. The energy release in each interval is calculated by:

$$\Delta H_i = \frac{AF_i}{Rm} \qquad (20)$$

where A is the area between the ΔT-T curve for the first heating cycle and the average of subsequent scans and F_i is the average DSC sensitivity factor over the interval integrated.

5.3.1.3 Accuracy of the DSC Measurements

The measurement of the release of stored energy by the DSC is based on determining the difference in thermal behavior of the specimen between two heating cycles. The first scan results in release of the stored energy, and the second scan provides a baseline representing the behavior of the specimen without stored energy. The assumptions are made that the entire stored energy is released in the first cycle and that no events occur as a result of the first cycle which alter the thermal behavior of the specimen, i.e., that the heat capacity remains the same and that no irreversible changes occur in the composition or structure of the specimen other than those associated with the release of the stored energy.

Failure of those assumptions to hold will result in errors of a systematic nature. The other potential source of systematic error is in the determination of the DSC sensitivity factor. The contribution of the systematic error to the uncertainty of the measurement was not estimated, but the close agreement between measurements made with both the drop calorimeter and the DSC indicate it is small compared with the random error.

The principal source of random error of the measurement is the lack of reproducibility of the base line. Shifts in the baseline are due mainly to random settling of the powdered sample in the sample pan resulting in changes of heat transfer characteristics between the sample and the calorimeter surroundings. The standard deviation of the measurement based on repeated runs of the same sample was estimated to be 2.0 cal $\cdot$ g^{-1}.

5.3.2 Drop Calorimetry

5.3.2.1 Design of the Drop Calorimeter

The design and operation of the drop calorimeter, Figure 5, has been previously described;[19] it was a Calvet-type microcalorimeter basically similar to that of Roux.[20] Measurements were made by holding the temperature of the calorimeter steady at the value of interest, and then dropping the sample into the calorimeter from a constant-temperature oven directly above the calorimeter. The quantity of heat absorbed by the sample was determined from the temperature transient observed on a 30-element Pt, Pt 10% Rh thermopile that read the difference between the inner calorimeter chamber receiving the specimen and a concentric alumina tube insulated from the inner chamber by about a 1/2 in. thickness of alumina powder. The thermopiles were wrapped on three 4-mm thick, alumina plates, 10 elements per plate. In accordance with Roux's technique, most of the signal resulting from normal heat capacity of a sample was bucked out by a "tapered-transmission-line," electrical analog simulator, to reduce the accuracy required for recording the temperature transient versus time information.

A movable pin supported the specimen in the oven above the calorimeter, and the specimen was dropped into the calorimeter by withdrawing this pin. The drop path was guided by a 2-ft-long ceramic tube closed at the bottom. The container was removed from the calorimeter by lowering a sleeve over it which was tapered so that the container became wedged within the sleeve. The sleeve was made of 10-mil nickel sheet and slit longitudinally so that it gripped the container by a spring-like action.

5.3.2.2 Calibration of the Drop Calorimeter

The area under the thermopile signal versus time plot was calibrated in terms of heat absorption using standard substances, alumina and platinum, in samples of different weights.*

---

* Similar measurements were used to determine heat pick-up of standard specimens (platinum encapsulated as described in Section 5.2.1) during the drop from the oven into the calorimeter. The experimental values of the heat pick-up depended, as expected, upon the temperature of the calorimeter T_h At T_h equal to 985°C, the pick-up was 0.6 cal. The pick-ups at lower calorimeter temperatures were less by approximately the amounts expected from considerations of the temperature dependence of radiative heat transfer.

ORNL-DWG 72-8123R2

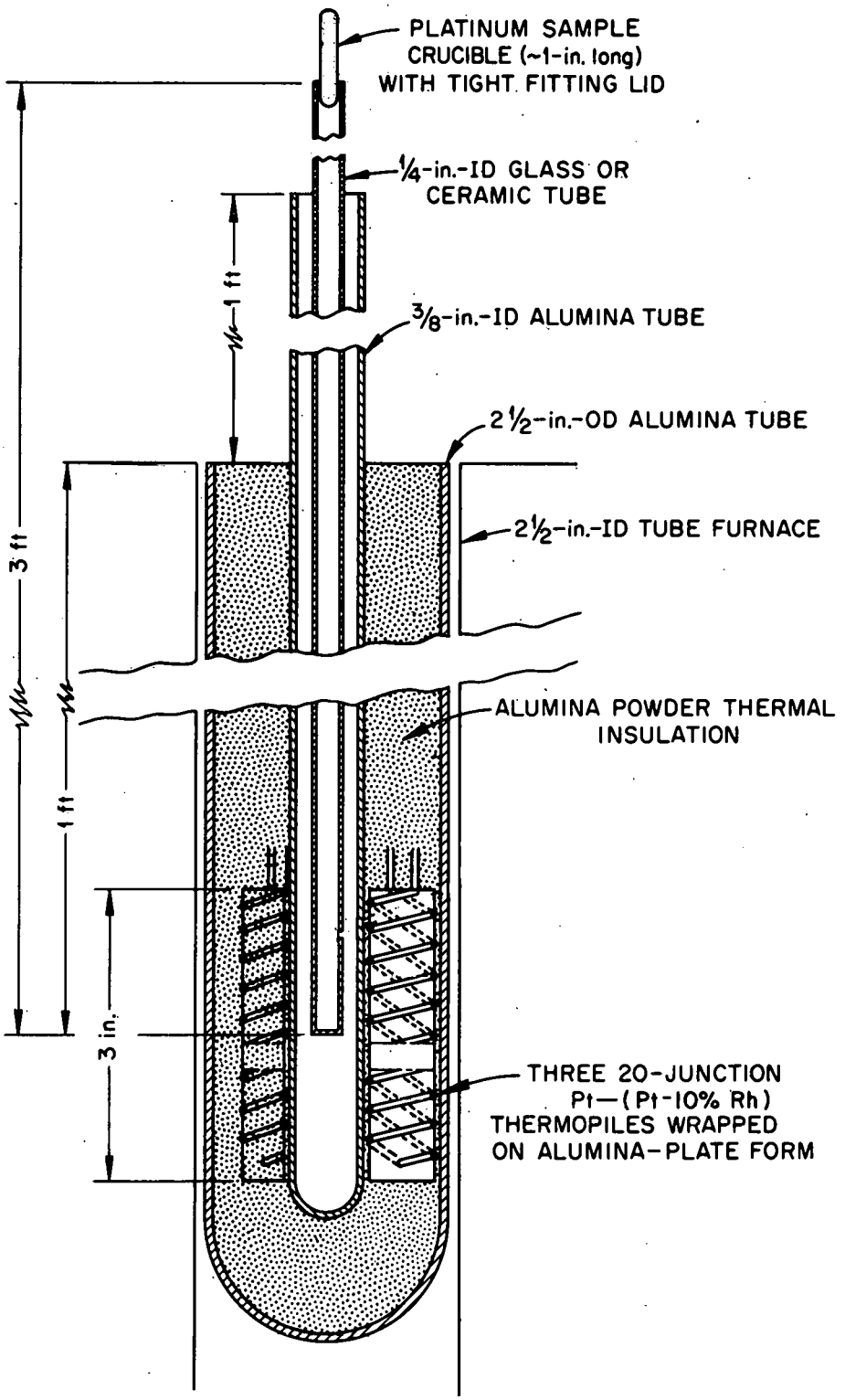

FIGURE 5. Roux-Type Drop Calorimeter

The temperature dependence of the calorimeter calibration from 195 to 1000°C fitted the empirical equation:

$$A = C[(T/428.6)^2 + 1]\,[\exp-(T/1605)^2] \qquad (21)$$

where

A is the area per unit energy absorbed

T is the calorimeter temperature in °K and

C is a constant independent of temperature.

The dependence of the value of A on temperature resulted primarily from changes in heat transfer between calorimeter parts with temperature, e.g., increases in radiative heat transfer between sample and drop tube and between drop tube and calorimeter liner (3/8-in. ID tube) with increasing temperature, and decreases in conductance across the thermopile plates with increasing temperature. Also, the thermoelectric power of the thermopile increased with increasing temperature.

The temperature transient versus time data did not conform to any simple mathematical relationship during the initial period after dropping a specimen. During the later part of transient decay, the decay followed Newton's law of cooling.* Conformance to this law was established or approximated about 10 to 15 min after the drop of a sample containing no stored energy, and 15 to 30 min after the drop of a sample containing stored energy. The area under the initial part of the transient was evaluated numerically. The later portions which obeyed Newton's law of cooling were evaluated using this law.

5.3.2.3 Accuracy of Drop Calorimeter Measurements

The principal source of error in the measurements at high temperature was drift in the furnace temperature over the period of about 10 to 30 min

* This law states that for small temperature differences the rate of loss of heat is proportional to the temperature above the surroundings. This law corresponds to an exponential decay of temperature; see Equations (22) and (23).

during which the temperature transient was measured. This drift was random in direction and amount. However, it increased with increasing calorimeter temperature. The effect of the drift was to change the zero point signal of the thermopile used to measure the transient (the zero point τ_0 was defined as the steady-state reading of the thermopile when no energy was being absorbed within the calorimeter). To take into account the change in τ_0 during a measurement, its value was estimated near the end of the 10 to 30 min period by choosing τ_0 to satisfy the equation:*

$$d(\tau - \tau_0)/dt = -k(\tau - \tau_0) \tag{22}$$

where τ is the thermopile signal, t is the time, and k is a constant. It was assumed that the change in τ_0 during a measurement occurred at a steady rate.

If it is assumed that τ_0 is constant in the time interval under consideration, Equation (22) can be integrated to

$$\ln(\tau - \tau_0) = -kt + \text{constant}. \tag{23}$$

The value of k was estimated using Equation (23) and data from several runs with samples containing no stored energy. It was assumed that τ_0 was the same as that at the start of a measurement, and semi-log plots of the data were made. The values for the slopes at 20 min were averaged to obtain the value of k. The value of k determined in this way was nearly independent of temperature in the temperature range in which measurements were made: 200 to 1000°C.

Our estimates of the accuracy of our measurements of heat content between T_i and T_h with the 0.2-g samples were ±0.04 cal and ±0.2 cal for annealed (no stored energy) samples in the temperature ranges 100 to 700°C and 700 to 1000°C, respectively. These values correspond to ±0.2 and ±1 cal/g, respectively. For samples containing stored energy, the estimated

---

* This equation follows from the assumption that the rate of heat flow is proportional to $\tau - \tau_0$.

accuracy was ±5% and ±15% of the stored energy in the temperature ranges 100 to 700°C and 700 to 1000°C, respectively. The uncertainties with the stored energy samples were, of course, never less than those for the annealed samples. As stated above, the accuracy of a measurement was primarily limited by the amount of drift of the calorimeter baseline, τ_o, during a measurement. The estimated accuracy was least for the samples containing stored energy because the release of stored energy during a measurement increased the time and therefore the baseline drift before the Newton's law extrapolation could be invoked.

6.0 EXPERIMENTAL RESULTS

6.1 ALPHA-IRRADIATED SPECIMENS

Nine specimens of the curium containing borosilicate glass (Melt 72-68) were allowed to self-irradiate and were measured at periodic intervals by the DSC to determine the enthalpy changes on heating from 23 to 600°C. Two of the specimens, A-4 and A-5 were devitrified as described in Section 5.1, and the remaining seven were vitreous.

Immediately after annealing, part of specimen A-27 was placed in a furnace held at 250° and allowed to self-irradiate at that temperature. Samples of A-3 were placed in furnaces held at temperatures ranging from 100 to 400°C after having accumulated a dose of 5.0×10^{17} α/g. The latter, measured once a week for 4 weeks after placing in the furnace, showed very little change in the quantity of stored energy from week to week. This indicated that annealing at the elevated temperature was complete within 1 week.

6.1.1 Stored Energy Release Behavior

The rates of energy release on heating as a function of temperature are shown in Figure 6a through 6j for the specimens held at room temperature. No sharp peaks are evident in the release curves although nearly all vitreous specimens show well defined maxima at 400 to 500°C. The maxima do not appear for the two devitrified specimens A-4 and A-5 (Figure 6b and 6c), and the maximum is much less pronounced in the vitreous specimen A-3 (Figure 6a).

The energy release is first detectable between 110°C and 125°C for the specimens irradiated and stored at room temperature. The release rate begins to decrease rapidly at about 450°C and is complete slightly below 600°C. The temperature at which the rapid decrease in the release rate occurs corresponds about to the softening point of the glass (about 500°C).

The stored energy release behavior is qualitatively similar for all of the alpha doses as seen in Figure 6i which shows the release curves for 5 different alpha doses for one specimen. The characteristic maximum, however, does shift to a lower temperature as the dose increases. Initially at 500°C the maximum drops to 450° at the highest dose.

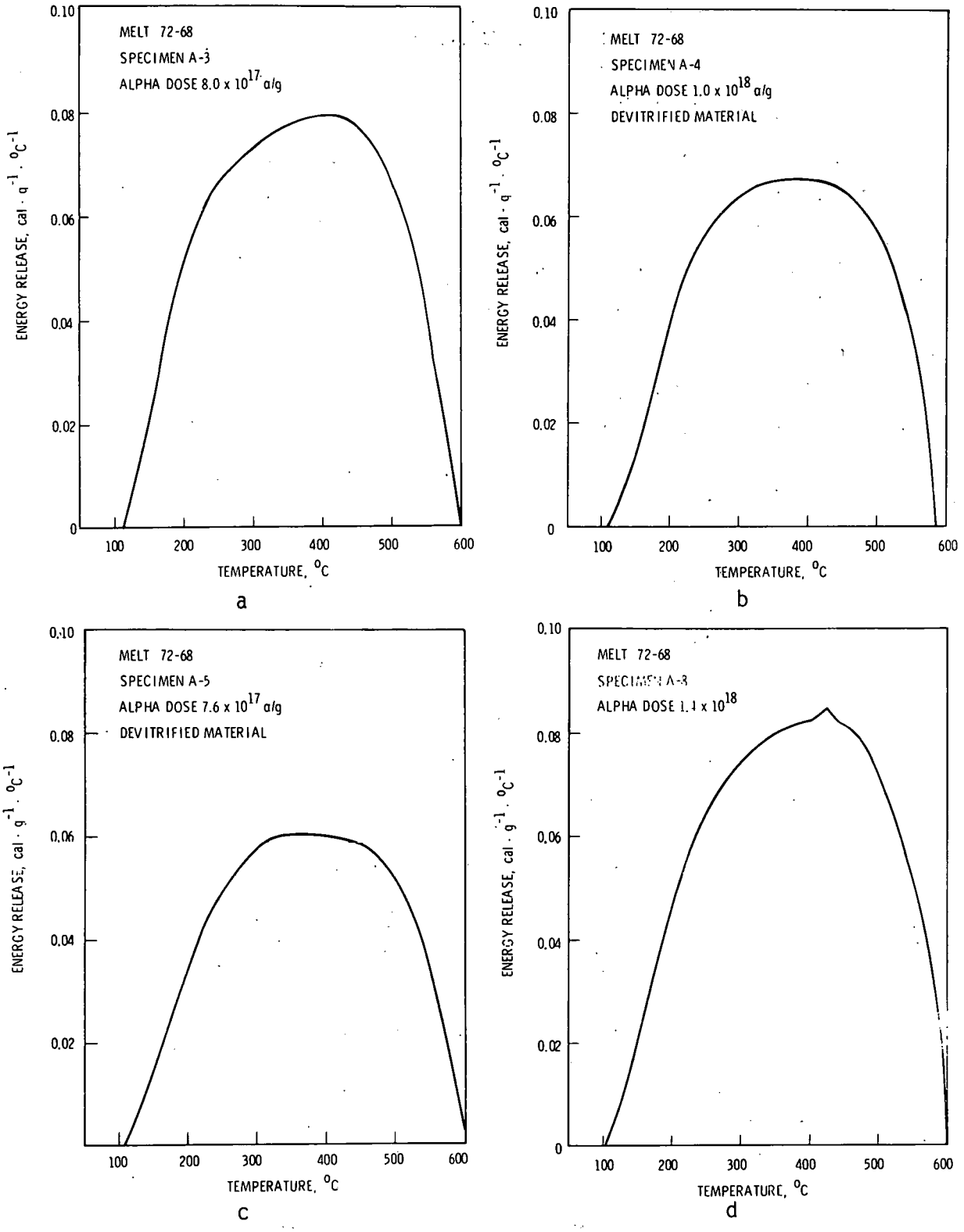

FIGURE 6. Energy Release Rates of Alpha-Irradiated Specimens

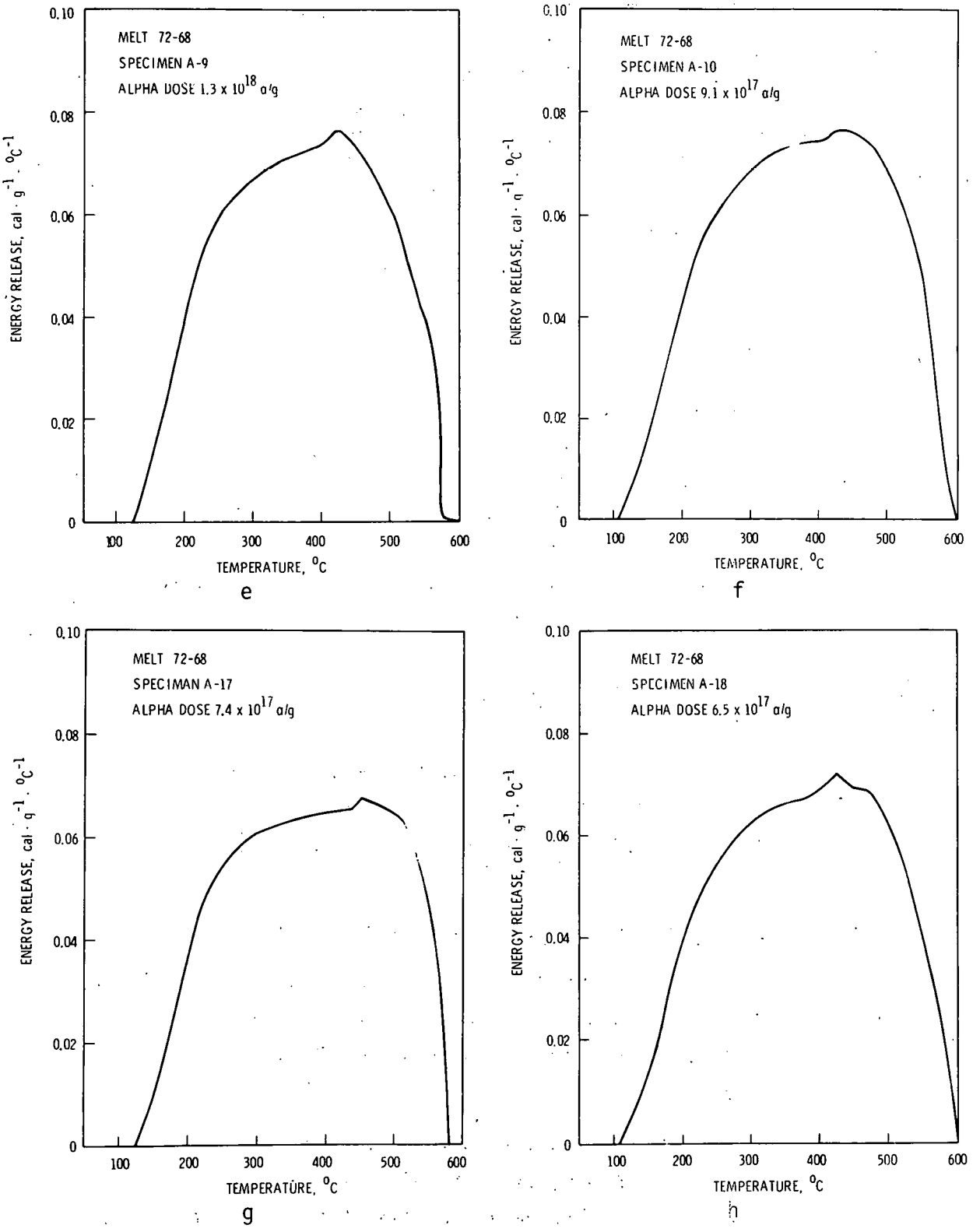

FIGURE 6. (contd)

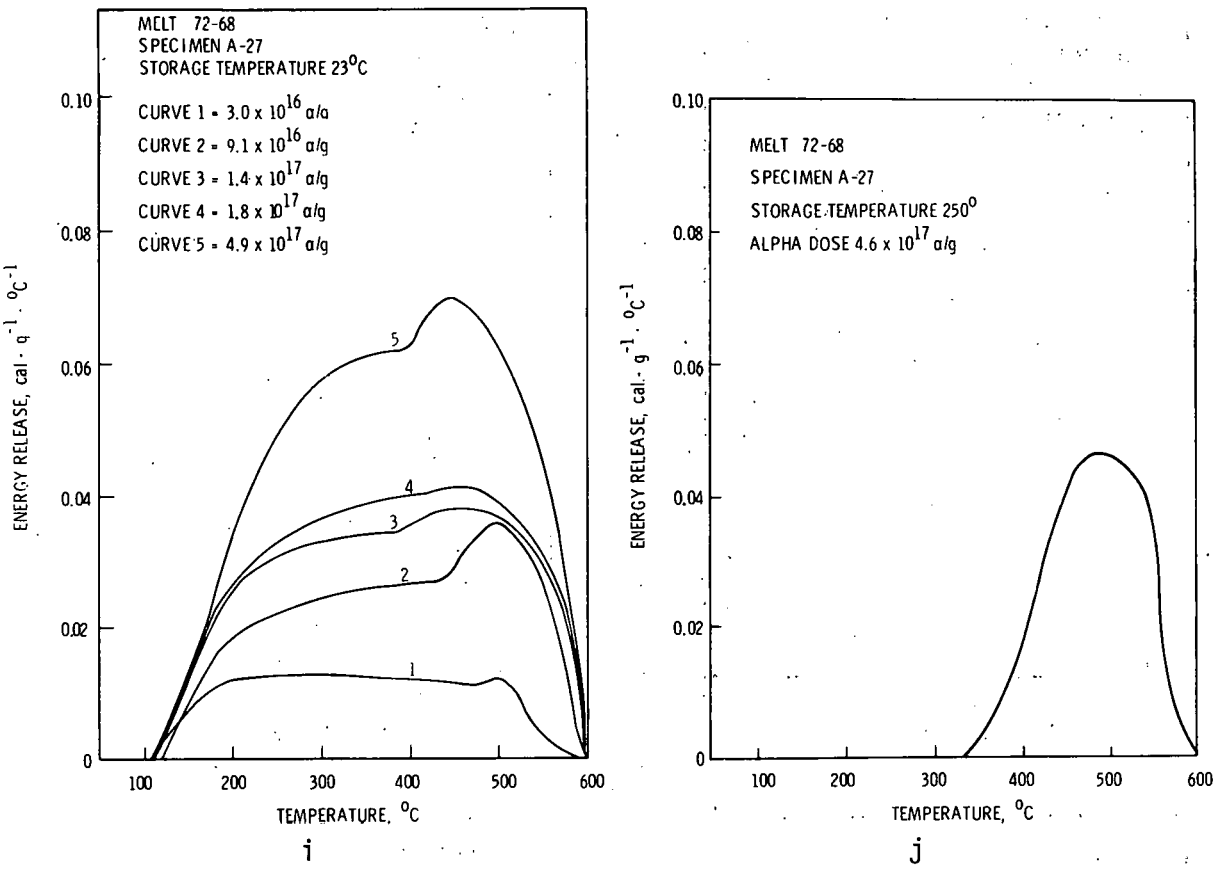

FIGURE 6. (contd)

Specimens irradiated or stored at elevated temperatures also behaved similarly except that the first detectable release occurred at higher temperatures. The initial release appeared at 75 to 125°C above the storage temperature (see Figure 6j).

6.1.2 Buildup of Stored Energy with Increasing Alpha Dose

The stored energy releases for the nine specimens held at room temperature were measured at various alpha doses accumulated over a 1-year period. The results of these measurements are shown in Figure 7 as a function of accumulated alpha dose.

The stored energy increases rapidly up to a dose of about 3×10^{17} α/g, reaching 17.5 cal/g. Near this dose the rate of increase diminishes and appears to approach saturation. The data indicate that the buildup is still

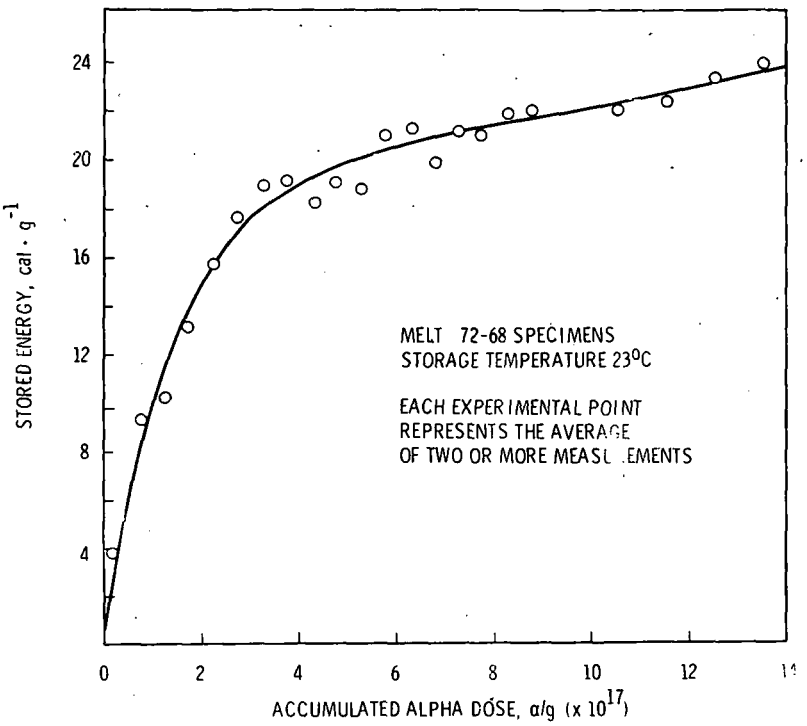

FIGURE 7. Buildup of Stored Energy with Alpha Dose

continuing even at 1.35×10^{18} α/g, the highest dose for which measurements were made. The stored energy was 23.5 cal/g at this dose.

The buildup of stored energy was also calculated in terms of storage time of solidified waste using the alpha activity in "real" waste from the reference UO_2 fuel (see Figure 1) and assuming a waste solidification process resulting in 168 kg glass per metric ton of fuel. The buildup as a function of storage time is shown in Figure 8. The highest dose for which measurements were made was equivalent to 780 years' storage.

6.1.3 The Effect of Storage Temperatures on Stored Energy

The stored energy for the specimen stored at 250° is shown in Figure 9 for various alpha doses up to 4.6×10^{17} α/g. The stored energy reached 6.5 cal/g at this storage temperature compared with 19.6 cal/g for the specimens stored at room temperature at the same dose. The buildup of stored energy is rapid at the lower alpha doses and gradually levels at the higher doses, displaying behavior similar to that of the specimens stored at room temperature.

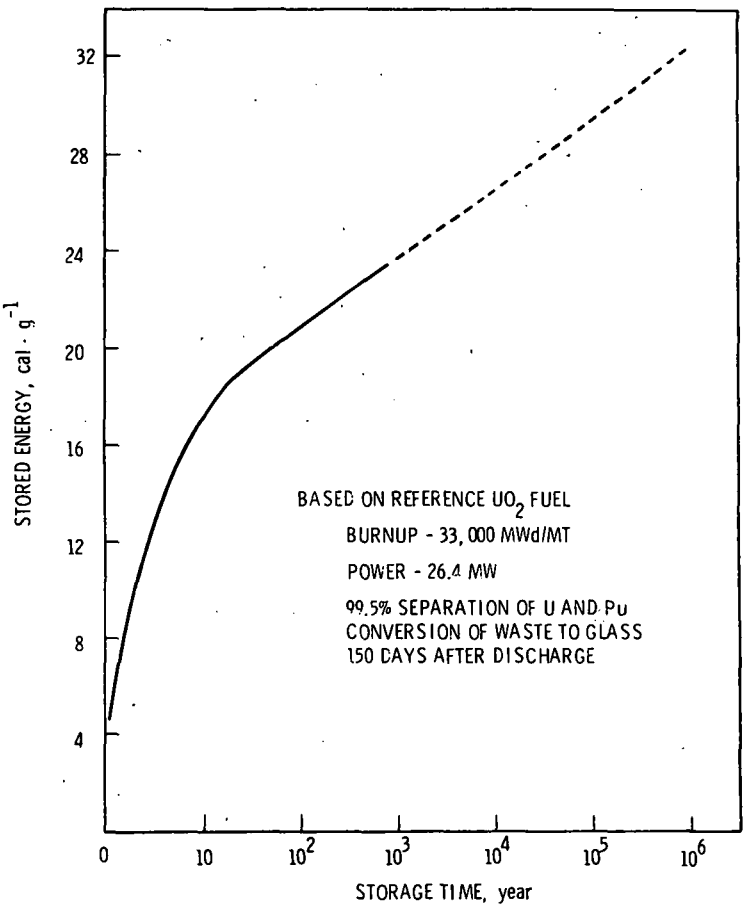

FIGURE 8. Stored-Energy Buildup with Age of Waste

Samples of A-3 held at various elevated temperatures for 4 weeks showed a nearly linear decrease in stored energy with increasing temperatures. As seen in Figure 10, annealing of the stored energy begins well below 100°C and is complete at about 350°C. This is quite different from the observed behavior on heating at 20°C/min during the DSC runs in which the release is not complete until nearly 600°C. (The residual stored energy versus sample temperature in the DSC is also plotted on Figure 10 for comparison.) The difference between the equilibrium values obtained from the 4-week storage times and the values obtained with rapid heating is due to the relatively slow annealing of the radiation damage in these specimens.

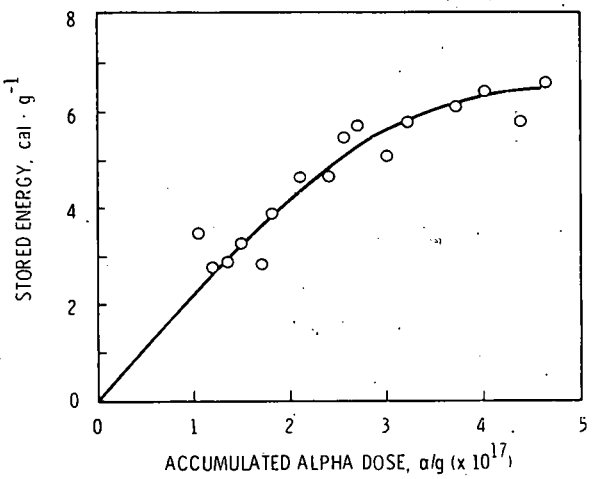

FIGURE 9. Build-Up of Stored Energy with Alpha Dos for Specimens Held at 250°C

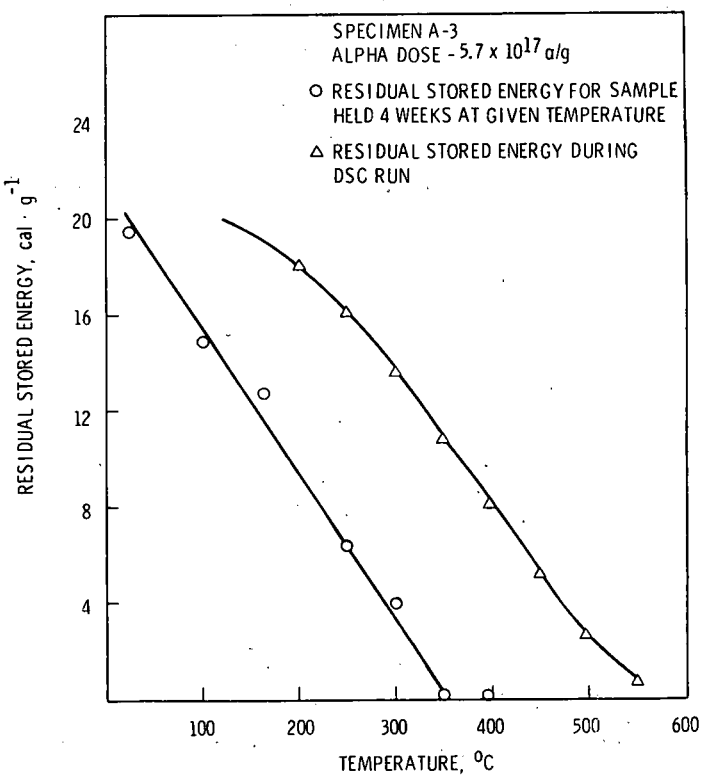

FIGURE 10. Annealing of Stored Energy

6.2 NEUTRON-IRRADIATED SPECIMENS

6.2.1 Presentation of Data

Tables 11 and 12 list the observed changes in enthalpy in the neutron-irradiated specimens upon heating to certain temperatures in the drop calorimeter (see Section 5.3 for definitions). The initial temperature was about 125°C in each case. The maximum experimental temperature obtained with a given material, other than the borosilicate glasses, was as high as appeared feasible. Factors which limited this temperature included swelling of the platinum capsules upon heating, large thermal effects with control specimens, and calorimeter limitations. The softening temperatures for the borosilicate glasses were 500 and 540°C for SEN-4 and SEN-5, respectively. Accordingly, we could assume that rapid annealing of all stored energy would take place at ~500°C.

The actual maximum temperatures in the drop calorimetry of specimens containing appreciable stored energy may have momentarily exceeded that of the calorimeter if the stored energy was released rapidly upon heating. For example, release of 20 cal/g of stored energy under adiabatic conditions would increase the temperature of a platinum-encapsulated borosilicate glass specimen by about 60°C.

The observed changes in enthalpy of unirradiated specimens upon heating in the drop calorimeter are shown in Table 13.

The experimental values for the average heat capacity in the temperature range 125°C to T_h (see Section 5.3 for definition) of irradiated specimens after annealing in the DC are included in Tables 11 and 12. Heat capacity values for unirradiated specimens of the glasses and alumina after heating to T_h in the DC are also shown. The experimental curves for the unirradiated specimens of the other materials in the DC were not evaluated in terms of heat capacity because we considered it likely that there would be no difference between irradiated and unirradiated specimens of these materials.

TABLE 11. Enthalpy Change of 12-Week Irradiated Specimens upon Heating, and Average Heat Capacity of Irradiated and Unirradiated Specimens After Annealing; Drop Calorimeter

Sample No. and Material	Calorimeter Temp., T_h, °C	ΔH(125°) cal/g	Average Heat Capacity Between 125° and T_h, cal/g/°C	
			Irradiated	Unirradiated
SEN-1 Calcine on Al_2O_3	670[a]	12	0.219	
	748[a]	1	-	
	714	15	0.213	
	748	11	0.220	
SEN-2 Calcine	887	17	0.140	
	887	14	0.138	
SEN-3 Al_2O_3	748[a]	10	0.270	0.271[b]
	809[a]	0	0.272	
	988	16.5	0.275	0.278[b]
	988	20.5	0.279	
SEN-4 Glass	489	18.5	0.220	
	506	23.5	0.208	0.238 ± 0.004[c] (510°)
	538	18	0.240	
SEN-5 Glass	489	17	0.202	
	506	21	0.202	0.202 ± 0.004[c] (510°)
	538	18	0.203	
SEN-7 Hot press	668[a]	30	0.208	
	714[a]	0	0.200	
	714	28	0.202	
	809	34	0.219	
SEN-9 Silica glass	809	30	0.261	0.260[d]
	988	32	0.260	0.266[d]
	988	34	0.261	0.265[e]

a. These samples measured sequentially at successively higher temperatures. All other samples measured at only one temperature.
b. Literature values.[21,23] Our measured values for unirradiated, annealed or unannealed agreed within experimental uncertainty with literature values.
c. Deviation between duplicate specimens.
d. Literature value.[22-24]
e. Measured value.

TABLE 12. Enthalpy Change of 6-Week Irradiated Specimens upon Heating, and Average Heat Capacity Irradiated and Unirradiated Specimens After Annealing; Drop Calorimeter

Sample No. and Material	Calorimeter Temp., T_h, °C	$\Delta H(125)$ cal/g	Average Heat Capacity Between 125°C and T_h, cal/g/°C	
			Irradiated	Unirradiated
SEN-1				
Calcine on Al_2O_3	512	6		
	743(a)	15		
	743(a)	10		
	968(a)	2		
SEN-2	897	21		
Calcine	897(a)	14		
	975(a)	11		
SEN-3	978	12		(b)
Al_2O_3	978	8		
SEN-4	333	7	0.229	
Glass	510	16	0.218 ± 0.003(c)	(b)
	510	22		
SEN-5	334(a)	7	0.196	
Glass	375(a)	1	0.202	
	482(a)	6	0.202	
	510	20	0.206 ± 0.002(c)	(b)
	510	20		
SEN-7				
Hot press	838	24		
	838	32		
SEN-9	977	35		
Silica glass	977	37		(b)

a. These samples measured sequentially at successively higher temperatures. All other samples measured at only one temperature.
b. See Table 11.
c. Deviation between duplicate specimens.

TABLE 13. Enthalpy Change upon Heating Unirradiated Specimens: Drop Calorimeter

Sample Number	Calorimeter Temp., T_h, °C	$\Delta H'(125)$ cal/g[a]
SEN-1	840	-3 ± 1
SEN-2	850-1000	13 ± 2[b]
SEN-3	978	<1
SEN-4	510	4 ± 0.1
SEN-5	510	2 ± 0.1
SEN-7	~840	-4 ± 1[c]
SEN-9	977	<1

a. The plus-minus values show the deviation from the average of duplicate samples.
b. Average and deviation for four samples in the temperature range 850 to 1000°C.
c. Measurements at calorimeter temperatures above and below 838°C gave this value within about 10%.

Table 14 gives the average heat capacity of the glass samples calculated from the second drop heat absorption data at low DC temperatures. The deviations from the mean between duplicate samples are shown for the unirradiated materials. Only a single sample of each of the irradiated materials was measured. The difference between enthalpies before and after heating to 195°C in the DC (not shown) was less than 0.1 cal/g in all cases, showing that annealing of stored energy was negligible during these measurements.

The differential thermograms obtained with the DSC for each unirradiated specimen are shown in Figures 11-16. These are plots of ΔT versus sample temperature from the sequential scans of the same sample. Differences between the first and the second scan indicate the occurrence of irreversible events. The DSC measurements made on the irradiated specimens are presented in Figures 17-23. These are plots of dH/dT versus sample temperature and show quantitatively the rate of release of heat as a function of sample temperature.

TABLE 14. Effect of Irradiation on the Average Heat Capacity of Glass Samples Measured Below the Annealing Temperature, Drop Calorimeter

Sample Number	Average Heat Capacity from 75 to 195°C, cal/g/°C	
	Before Irradiation	After Irradiation[a]
SEN-4	0.203 ± 0.001	0.204[b]
SEN-5	0.182 ± 0.003	0.166[b]
SEN-9	0.222 ± 0.004	0.216[c]

a. 12-week irradiation.
b. For comparison, the experimental values in the temperature range 125 to 510°C were 0.238 and 0.202 for SEN-4 and SEN-5, respectively. See Tables 11 and 12.
c. The literature[24] value for fused silica between 75 and 195°C is 0.211.

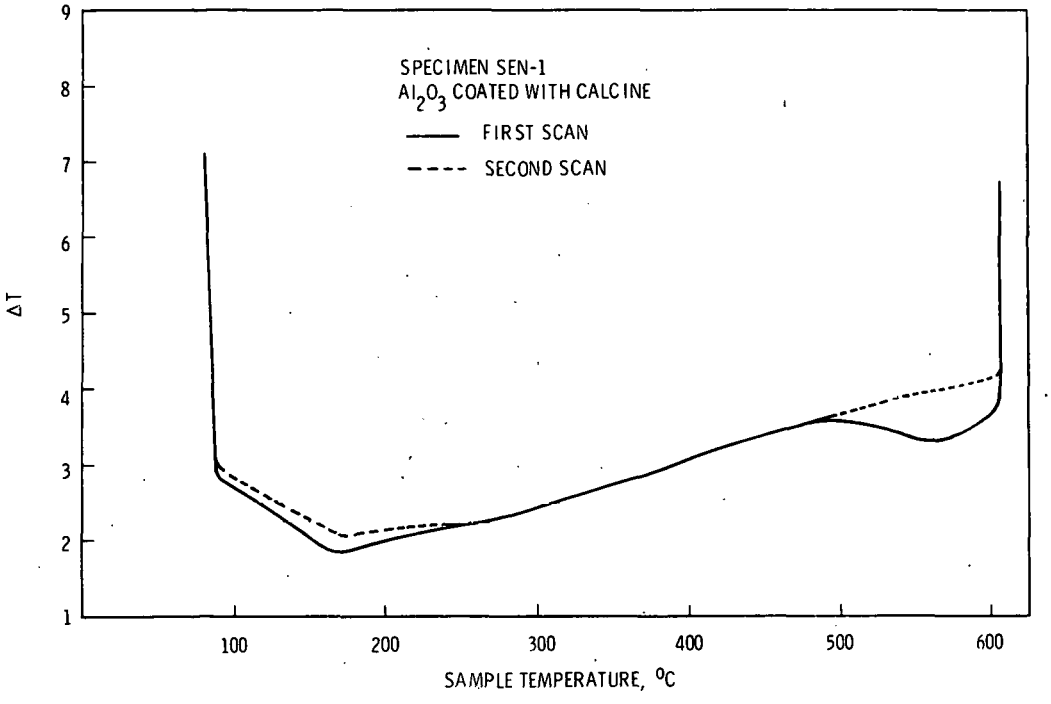

FIGURE 11. ΔT Versus Temperature for Unirradiated SEN-1

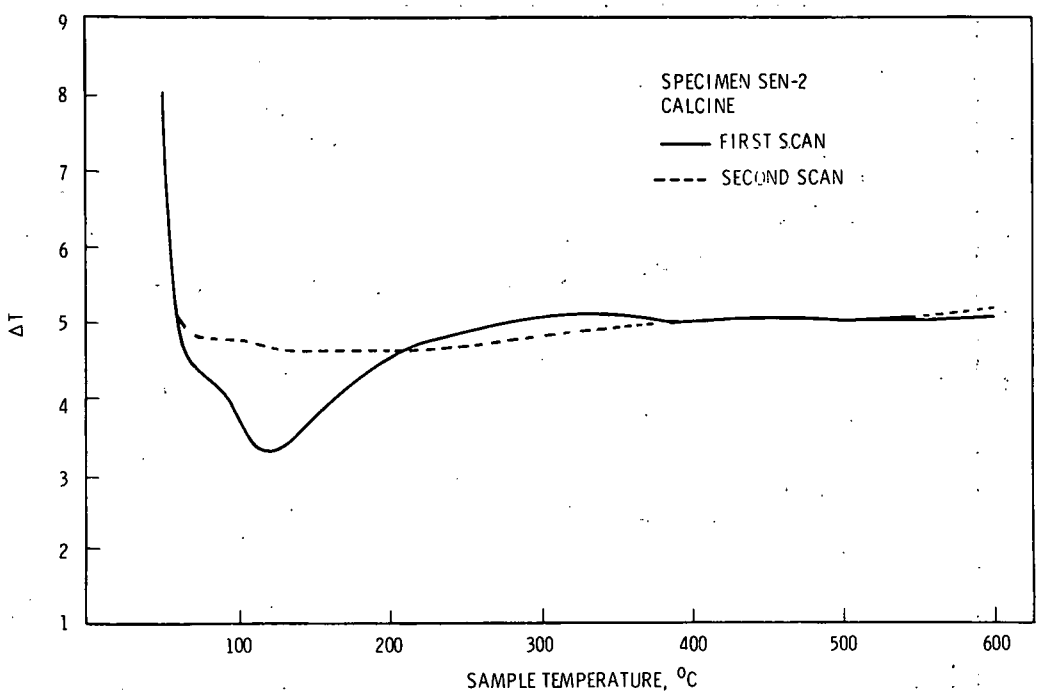

FIGURE 12. ΔT Versus Temperature for Unirradiated SEN-2

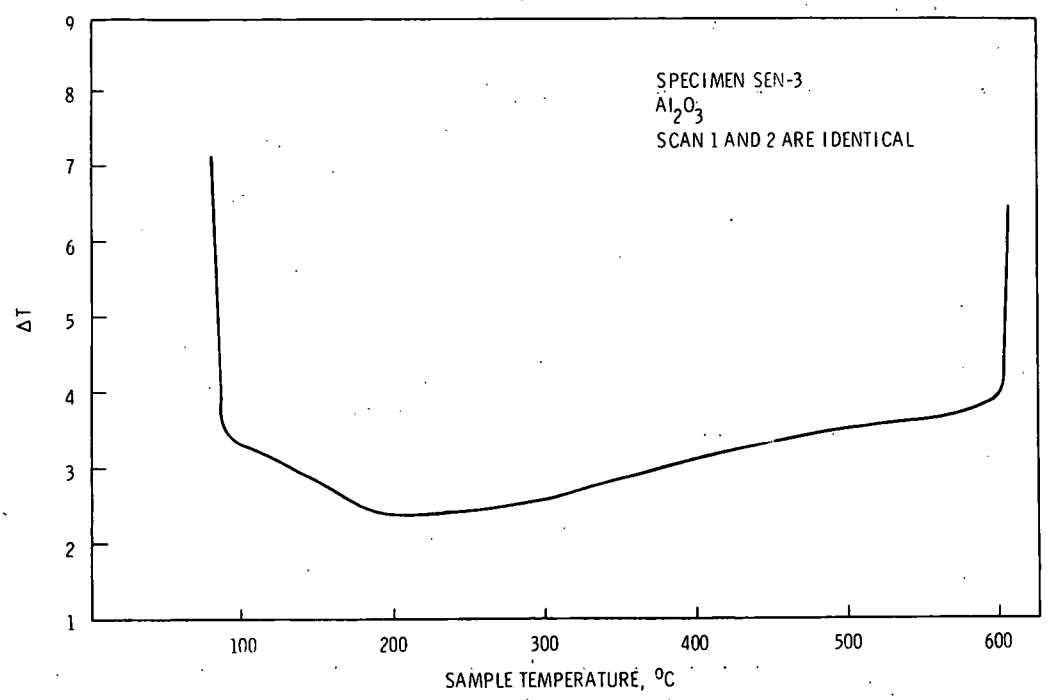

FIGURE 13. ΔT Versus Temperature for Unirradiated SEN-3

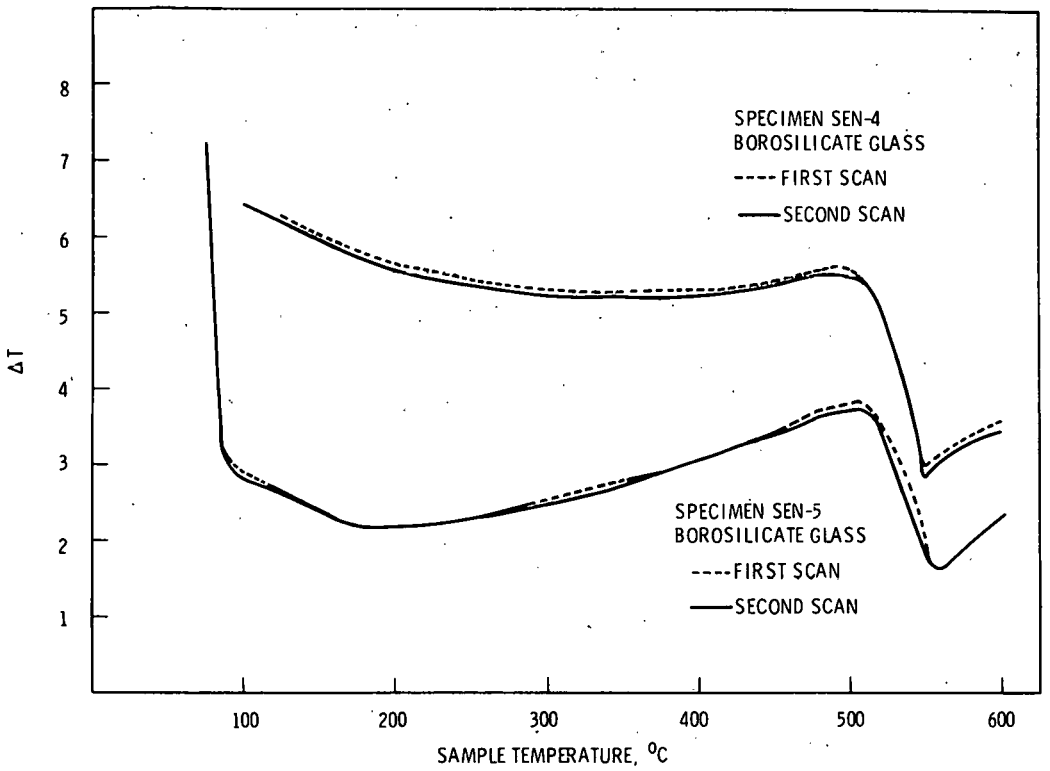

FIGURE 14. ΔT Versus Temperature for Unirradiated SEN-4 and SEN-5

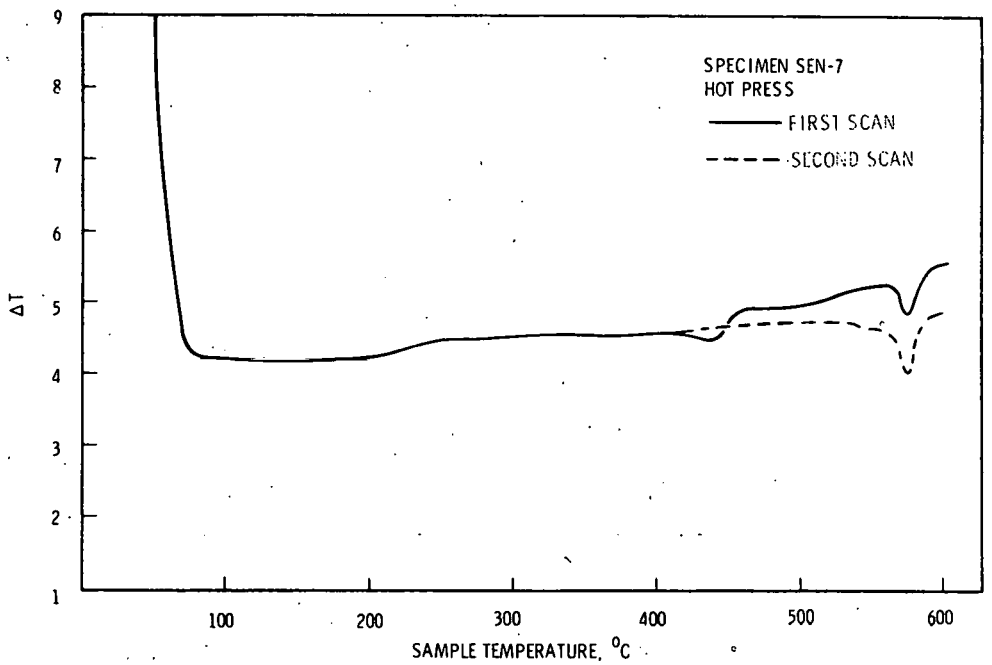

FIGURE 15. ΔT Versus Temperature for Unirradiated SEN-7

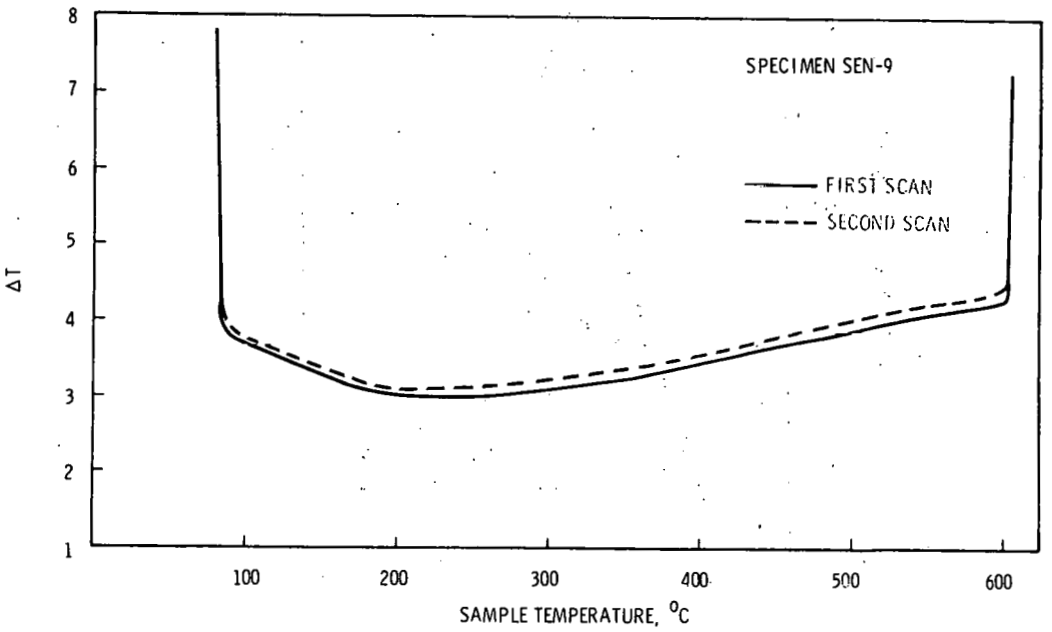

FIGURE 16. ΔT Versus Temperature for Unirradiated SEN-9

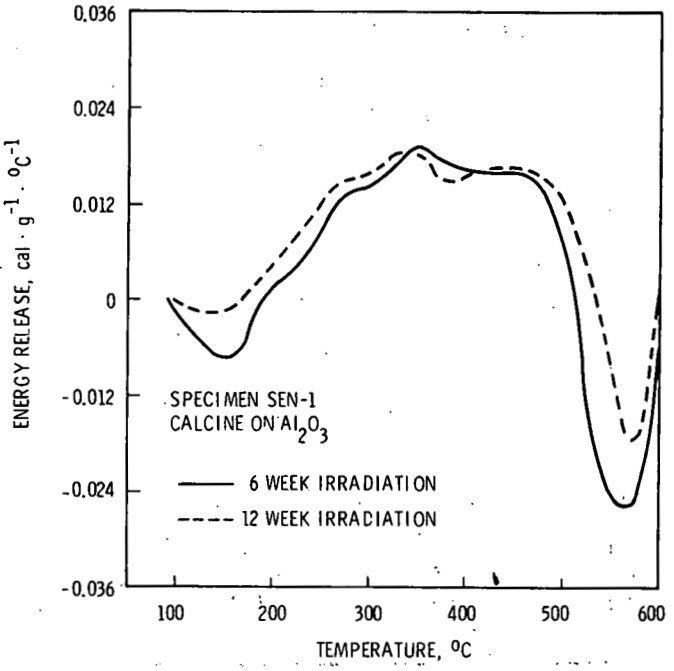

FIGURE 17. Energy Release Rate Versus Temperature for Neutron-Irradiated SEN-1

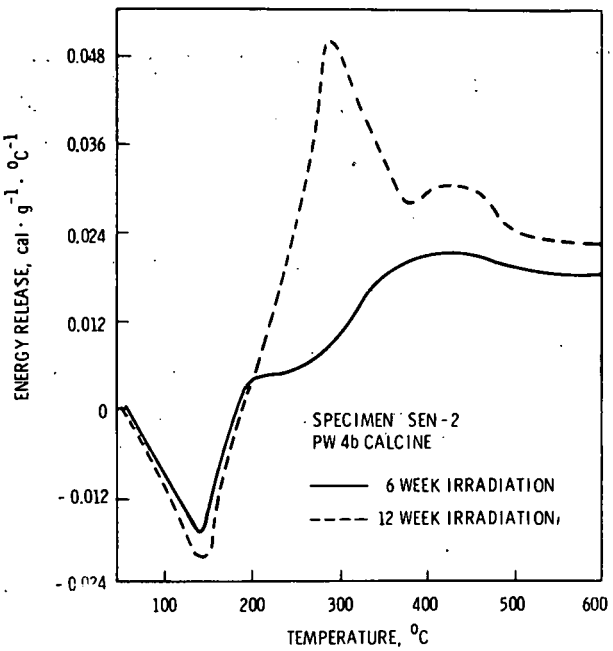

FIGURE 18. Energy Release Rate Versus Temperature for Neutron-Irradiated SEN-2

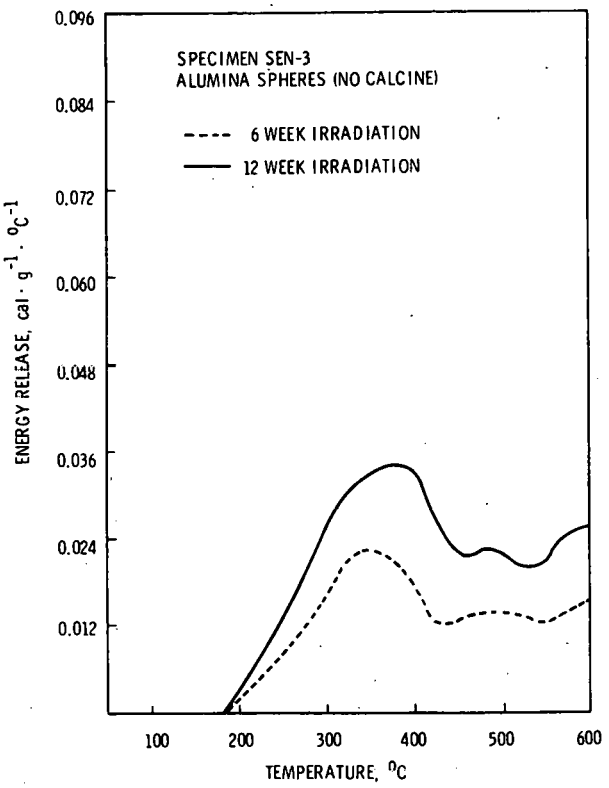

FIGURE 19. Energy Release Rate Versus Temperature for Neutron-Irradiated SEN-3

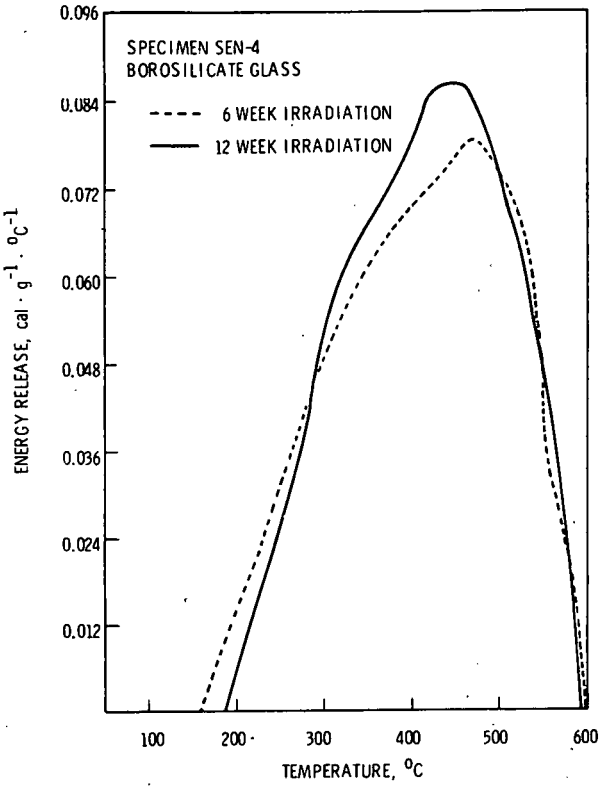

FIGURE 20. Energy Release Rate Versus Temperature for Neutron-Irradiated SEN-4

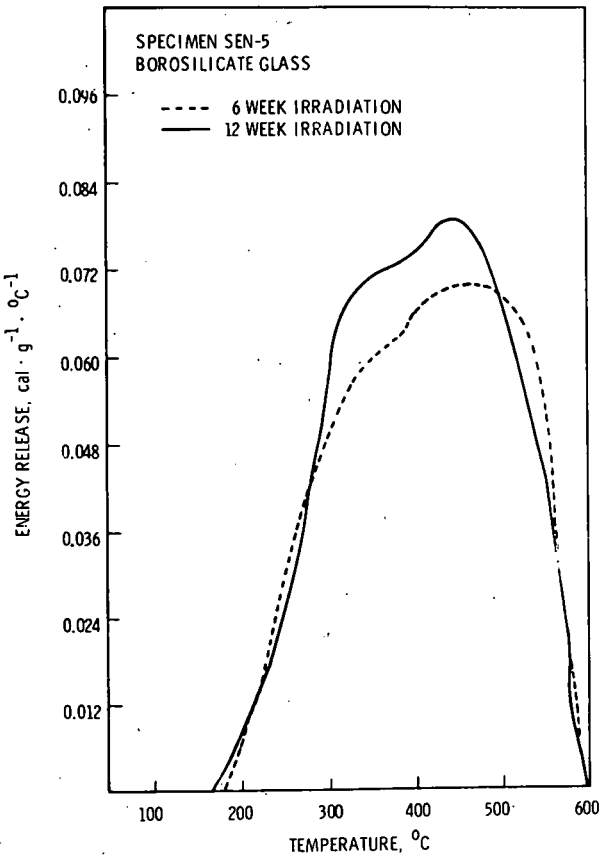

FIGURE 21. Energy Release Rate Versus Temperature for Neutron-Irradiated SEN-5

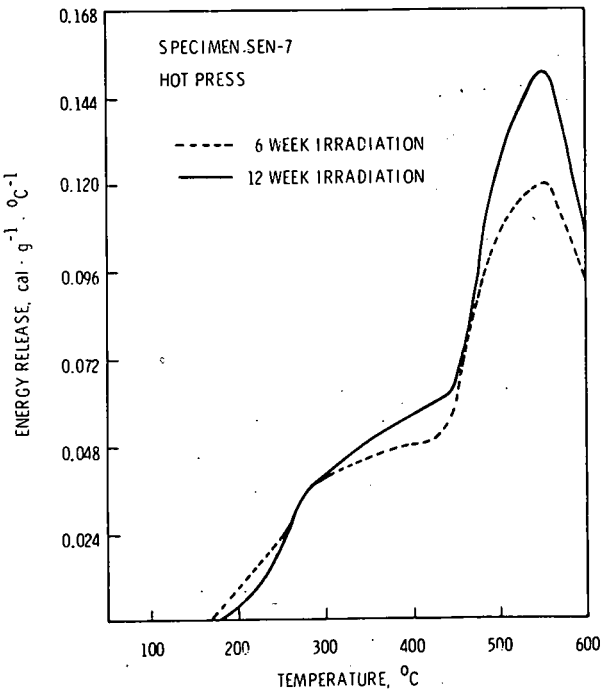

FIGURE 22. Energy Release Rate Versus Temperature for Neutron-Irradiated SEN-7

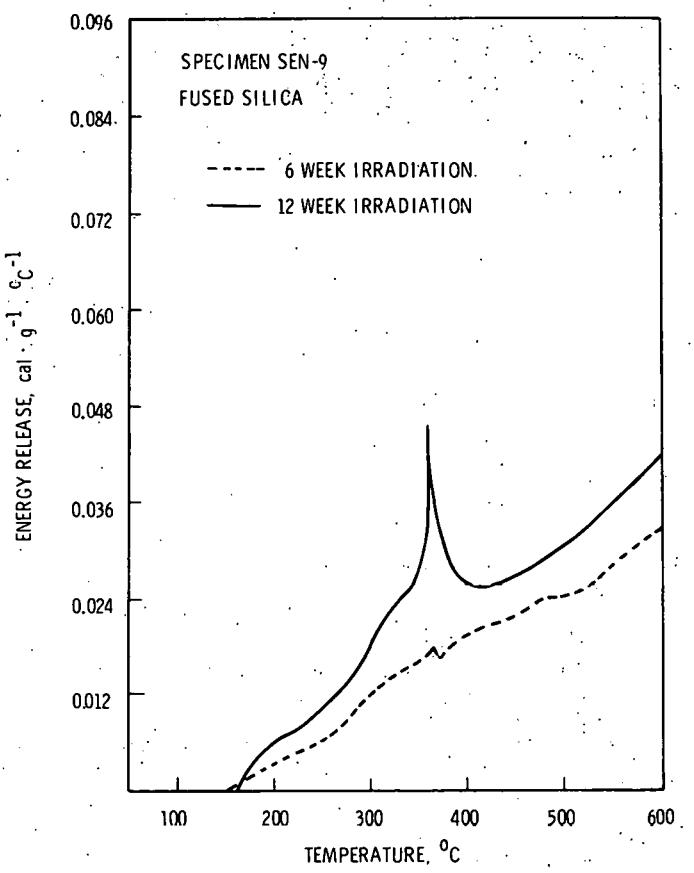

FIGURE 23. Energy Release Rate Versus Temperature for Neutron-Irradiated SEN-9

Values for total amounts of heat released within certain temperature intervals, obtained by integration of the DSC rate data, are included in Tables 15-22. The listed values are the average of the results of measurements on two samples where the results differed only slightly. Where there were appreciable differences between the two samples, both results are listed.

Heat release commenced between 160 and 200°C for all of the neutron-irradiated specimens. The two specimens containing calcine initially underwent an endothermic reaction below 200°C, as is evident from the negative values in the heat release rate curves (Figures 17 and 18). The calcine on alumina specimen also underwent an endothermic reaction in the temperature region of 500 to 600°C.

TABLE 15. Enthalpy Changes upon Heating and Ratios of the Values at Different Annealing Temperatures for Neutron-Irradiated Alumina

Investigator and Calorimeter Type	Annealing Temp., °C	Enthalpy Change, ΔH, and Ratio of Change to that Reported by Roux for Annealing at 1200 °C			
		Fluence > 1 MeV(a) 1.45×10^{20}		Fluence > 1 MeV(a) 3.48×10^{20}	
		ΔH	Ratio	ΔH	Ratio
Present; DSC	350(b)	2.1	0.13	2.9	0.11
Present; DSC	400(b)	3.0	0.18	4.1	0.15
Present; DSC	600(b)	5.6	0.34	8.5	0.32
Present; DC	750	-	-	10	0.37
Present; DC	978-988	12	0.73	16.5	0.62
Present; DC	978-988	8	0.48	20.5	0.77
Roux; DC(c)	1200	16.5	1	26.7	1

a. The neutron fluences employed by Roux [20] were 1.5×10^{20} and 3.2×10^{20}, cm^{-2}, >1 MeV. His specimen temperatures during irradiation were about 100°C.
b. ΔH values are for heat released in temperature range below this temperature.
c. Reference 20.

TABLE 16. Enthalpy Changes upon Heating and Ratios of the Values Measured at Different Temperatures for Neutron-Irradiated Fused Silica

Calorimeter Type	Annealing Temp., °C	Enthalpy Change, ΔH, and Ratio of Change to that Measured at 977-988°C			
		Fluence > 1 MeV 1.45×10^{20}		Fluence > 1 MeV 3.48×10^{20}	
		ΔH	Ratio	ΔH	Ratio
DSC	350(a)	1.4	0.04	2.4	0.07
				2.9	0.08
DSC	400(a)	2.2	0.06	4.0	0.11
				4.7	0.13
DSC	600(a)	7.0	0.20	9.9	0.28
				13.2	0.38
DC	809	-	-	30	0.86
DC	977	35	1	-	-
DC	977	37	1	-	-
DC	988	-	-	32	1
DC	988	-	-	34	1

a. ΔH values are for heat released in temperature range below this temperature.

TABLE 17. Enthalpy Changes Observed upon Heating Samples of Calcine, SEN-2

Calorimeter Type	Annealing Temp., °C	Enthalpy Change in Irradiated Specimens, cal/g[a]	
		Fluence > 1 MeV 1.45×10^{20}	Fluence > 1 MeV 3.48×10^{20}
DSC	400[b]	2.6	6.2
DSC	600[b]	6.2	11.3
DC	897	21	-
DC	897[c]	14	-
	975[c]	11	-
DC	887	-	17
DC	887	-	14

a. $\Delta H'$ equaled 13 cal/g at T_h = 850 to 1000°C in DC measurements. In DSC measurements on unirradiated specimens, 1.4 cal/g was released in the temperature range 205 to 600°C.
b. ΔH values are for heat released in temperature range between 205°C and this temperature.
c. These samples measured sequentially at successively higher temperatures.

TABLE 18. Enthalpy Changes Observed upon Heating Samples of Calcine on Alumina, SEN-1

Calorimeter Type	Annealing Temp., °C	Enthalpy Change in Irradiated Specimens, cal/g[a]	
		Fluence > 1 MeV 1.45×10^{20}	Fluence > 1 MeV 3.48×10^{20}
DC	512	6	-
DSC	400[b]	2.6	2.9
DSC	500[b]	3.8	4.4
DSC	600[b]	4.4	4.5
DC	743	15	-
DC	743[c]	10	-
	968[c]	2	-
DC	670[c]	-	12
	748[c]	-	1
DC	714	-	15
DC	748	-	11

a. $\Delta H'(125)$ equaled -3 cal/g at T_h equal to 840°C in DC measurements. In DSC measurements on unirradiated specimens, 2.5 cal/g were absorbed in the temperature range 480 to 600°C.
b. ΔH values are for heat released in temperature range 180°C to this temperature.
c. These samples were measured sequentially at successively higher temperatures.

TABLE 19. Enthalpy Changes Observed upon Heating Samples of Hot Press, SEN-7

Calorimeter Type	Annealing Temp., °C	Enthalpy Change in Irradiated Specimens, cal/g[a]	
		Fluence > 1 MeV 1.45×10^{20}	Fluence > 1 MeV 3.48×10^{20}
DSC	400[b]	7.0 8.1	7.3
DSC	600[b]	25.1 28.3	30.2
DC	838	32	-
DC	668[c] 714[c]	- -	30 0
DC	714	-	28
DC	804	-	34

a. $\Delta H'(125)$ equaled -4 cal/g at T_h equal to 838°C in DC measurements. In DSC measurements of unirradiated specimens, a net heat release of 4.5 cal/g was observed between 425 and 600°C, Figure 4.
b. ΔH values are for heat released in temperature range below this temperature.
c. These samples were measured sequentially at successively higher temperatures.

TABLE 20. Enthalpy Changes Observed upon Heating Samples of Borosilicate Glass, SEN-4

Calorimeter Type	Annealing Temp., °C	Enthalpy Change in Irradiated Specimens, cal/g[a]	
		Fluence > 1 MeV 1.45×10^{20}	Fluence > 1 MeV 3.48×10^{20}
DC	333	7	-
DSC	350[b]	5.1	5.7
DSC	400[b]	9.5	9.5
DSC	500[b]	16.9	18.1
DC	489	-	18.5
DC	506	-	23.5
DC	510	22	-
DC	510	16	-
DC	538	-	18
DSC	600[b]	20.7	22.6

a. $\Delta H'(125)$ = 4 cal/g at T_h = 510°C in DC measurements. In DSC measurements there were no irreversible thermal effects.
b. ΔH values are for heat released in temperature range below this temperature.

TABLE 21. Enthalpy Changes Observed upon Heating Samples of Borosilicate Glass, SEN-5

Calorimeter Type	Annealing Temp., °C	Enthalpy Change in Irradiated Specimens, cal/g[a]	
		Fluence > 1 MeV 1.45×10^{20}	Fluence > 1 MeV 3.48×10^{20}
DC	334[b]	7	-
	375[b]	1	-
	482[b]	6	-
DSC	350[c]	5.6	6.0
DSC	400[c]	8.7	9.2
DSC	500[c]	15.5	16.5
DC	489	-	17
DC	506	-	21
DC	510	20	-
DC	510	20	-
DC	538	-	18
DSC	600[c]	19.7	19.5

a. $\Delta H'(125) = 2$ cal/g at $T_h = 510°C$ in DC measurements. In DSC measurements, there were no irreversible thermal effects.
b. This sample was measured sequentially at successively higher temperatures.
c. ΔH values are for heat released in temperature range below this temperature.

TABLE 22. Average Heat Capacity Observed in Samples of SEN-4 and SEN-5

Temperature Range, °C	Quantity Measured[a]	Average Heat Capacity cal/g/°C	
		SEN-4	SEN-5
75-195	C'_1 (unirradiated)	0.203	0.182
75-195	C_1 (irradiated 12 weeks)	0.204	0.166
125-510	C'_2 (unirradiated)	0.238	0.202
125-510	C_2 (irradiated 6 weeks)	0.218	0.206
125-510	C_2 (irradiated 12 week)	0.208	0.202

a. See Section 5.3 for definition.

The energy releases observed in the DSC measurements were complete at 600°C (the highest temperature used) only for the two borosilicate glasses SEN-4 and SEN-5. The rest of the specimens continued to evolve heat at 600°C, and complete release was obviously not attained in these cases. However, when heating was discontinued and the calorimeter temperature was fixed at 600°C, the ΔT value quickly returned to zero, showing that the remainder of the stored energy was being annealed very slowly (or not at all) at this temperature.

6.2.2 Discussion of Results with Neutron-Irradiated Specimens

Given here are comments on the interpretations of the experimental results and on comparisons with those reported by other workers.

Other workers have studied neutron-irradiation effects on both alumina and silica, and considerable information is available on the growth and thermal annealing of stored energy and of density changes for these materials. No reported experimental information is available on radiation effects in the other sample materials.

SEN-3, Alumina Spheres

The results of our measurements of enthalpy changes upon heating neutron-irradiated specimens of alumina are assembled in Table 15. Also included are results reported previously by Roux[20] for specimens of sintered alumina which were irradiated at comparable fluences and temperatures and then analyzed for enthalpy change with a drop calorimeter operating at 1200°C. Several features of the results are noted:

1. Saturation of stored energy was not reached at the maximum neutron fluences tested--3 to 3.5 x 10^{20} > 1 MeV.
2. The ratios of the amounts of enthalpy change observed at the lower fluence to that at the higher were approximately independent of calorimeter (annealing) temperature at 600°C and above and about the same as that for Roux's reported data.

3. The observed changes in enthalpy increased with increasing annealing temperature as shown by the listed values for the ratio of our results to those reported by Roux.[20]

Considerations of reported literature information led us to conclude:

1. The differences between the amounts of enthalpy change observed at different calorimeter temperatures resulted from incomplete annealing of the stored energy below 1200°C (and possibly below 1400°C).
2. The total radiation-induced enthalpy changes in our specimens were near those reported by Roux.[20]
3. An estimate of about 50 cal/g for the total stored energy at approximate saturation can be made using a reported[20] relationship between radiation-induced enthalpy and density changes. Our considerations which led to these conclusions are discussed below.

First consider whether the difference between the amounts of enthalpy change reported by Roux and those found in this work might be ascribed to differences between sample materials and/or between neutron energy spectra. Germane to these considerations are 1) the report by Roux that there was a direct relationship between the enthalpy and the density changes which he observed in his irradiated specimens and 2) the results of studies of density changes induced in alumina by neutron irradiations at 60 to 100°C reported by several different investigators[25-27] using different sample materials and exposing their samples in several different reactors. Comparisons of these reported results indicated that there was no difference between the density change at a given fluence, >1 MeV, in the range under consideration in single crystals and in polycrystalline materials prepared in several different ways. Also there was no significant difference between results obtained with irradiations in the ETR or the HIFAR or the RA Reactor. The HIFAR is a tank

type reactor (Australian) using D_2O moderator. The ETR and the ORR are tank type reactors using H_2O moderator. Roux did not report the reactor in which his irradiations were made, but it can be inferred from reported work of others[26] that some or all of the Al_2O_3 irradiations were in the RA reactor at Vinca, Yugoslavia. This is also a tank type reactor with D_2O moderator. We concluded that possible differences between the sample materials and radiations sources did not account for the differences between the enthalpy changes reported by Roux and those found in our work.

Next consider the fractional annealing of stored energy at temperatures below 1200 to 1400°C. Reported information on the fractional annealing of radiation-induced density changes is pertinent here. Specifically, Hickman and Walker[25] reported studies of the annealing of radiation-induced density changes in single crystals of alumina in which specimens irradiated in the HIFAR Reactor were heated for 1 hr at consecutively higher temperatures between 200 and 1400°C in 200° steps. Their specimen temperatures during irradiation were 75 to 100°C and the neutron fluences >1 MeV were 4.4×10^{19} to 5.0×10^{20} cm^{-2}. Their results showed that the fractional annealing corresponded to 14%, 27%, 48%, 65%, and 90% after heating at 400, 600, 750, 1000, and 1200°C, respectively, and was independent of the fluence to which a specimen was exposed. Others[26] have shown that most of the annealing taking place at a given temperature occurs within a few tens of minutes after the initial exposure to the temperature.

The values for the fractional amounts of density-annealing at 400, 600, 750, and 1000°C mentioned in the preceding paragraph are near those, listed in Table 15, for the values of the ratio at these temperatures. Also, and in particular, the relative values of the ratios at a given fluence are near those for the relative amounts of density annealing at the respective temperatures. These agreements led us to infer that an approximate linear relationship between fractional amounts of thermal annealing of radiation-induced density changes and of stored energy in alumina prevails up to at least 1200°C. It also led to the conclusion mentioned above that most of the differences between Roux's and our stored energy data resulted from the differences between calorimeter temperatures.

On the basis of reported[25,27] effects of 70 to 100°C irradiations on density, it can be estimated that an approximate saturation of the density change at about 1.4% is reached at a fluence of about 1 x 10^{21} cr ^{2}, >1.0 MeV.* From Roux's relationship between stored energy and volume increase prior to annealing, it can be estimated that about 50 cal/g would be associated with the 1.4% volume increase.

SEN-9, Fused Silica

The results of the calorimetric measurements on fused silica are assembled in Table 16.

The amounts of stored energy measured at T_h equal to about 1000°C apparently reached saturation at about 35 cal/g during the 6-week irradiation. This agrees with the results of Roux[20] who reported that saturation was reached at a fluence of 3 x 10^{19}, >1 MeV. Our stored energy values, 31 to 37 cal/g, are within the range of values reported by Roux for high-fluence specimens. Roux's calorimeter temperature was also about 1000°C with the fused silica.

Just as for alumina, it is possible that the actual amounts of stored energy exceeded those measured at 1000°C. No direct information on this possibility is available. However, the results of others for the annealing of radiation-induced density changes in heavily irradiated fused silica indicated that a small fraction (5 to 15%) of the density change remained after heating for 30 min at 1000°C.[28,29] It seems likely that some stored energy also remained after the 1000°C DC measurements. Assuming this was also in the range 5 to 15%, the total radiation induced enthalpy changes in our specimens equaled about 40 cal/g.

There were small differences between the heat capacity between 125 and 980°C of irradiated and unirradiated specimens of fused silica after annealing at 980°C. These differences may have resulted from partial devitrification of the irradiated silica during annealing at 980°C. The heat capacity

* The volume continues to increase slowly with increasing fluence above 1 x 10^{21} cm^{-2}.(27)

of irradiated and unirradiated material in the temperature range 75 to 195° (see Table 14) did not differ significantly.

SEN-2, Calcine

The results of the various calorimetric measurements on the calcine are assembled in Table 17.

The net enthalpy changes in this material in the temperature region 200 to 600°C increased from 6.2 to 11.3 cal/g between the 6-week and 12-week irradiations, showing that stored radiation energy had not saturated at the radiation levels studied. Measurements at higher temperatures were not conclusive because of large thermal effects apparently unrelated to radiation damage. Unirradiated samples showed a large exotherm of +13 ± 2 cal/g occurred between 600 and 1000°C. The maximum enthalpy change in irradiated samples was 25 cal/g at 975°C (the sum released in the sequential runs at 897 and 975°C for the 6-week irradiation). No similar data are available at this temperature for the 12-week irradiation.

The unirradiated material also showed a small enthalpy change of +1.4 cal/g between 205 and 600°C (see Figure 12). In addition an endotherm occurred below 200°C, resulting in an enthalpy change of -4 cal/g. This endotherm was also observed in irradiated samples but was much smaller, amounting to only 1.5 cal/g.

The DC results with T_h = 897 to 975° also indicated a significant effect of irradiation on the enthalpy in the case of the 6-week specimens. The enthalpy changes upon heating in these cases increased by about 10 cal/g above the 13 cal/g which prevailed before irradiation. However, the enthalpy change upon heating the 12-week specimens in this higher temperature range amounted to only a few calories per gram above the preirradiation 13 cal/g.

The experimental results outlined above suggest that the radiation defects produced during the 6-week irradiation added to the disorder already present to result in the relatively large enthalpy changes during heating at 897 to 975°C. They also suggest that the longer irradiation caused some annealing of this disorder.

SEN-1, Al_2O_3 Coated with Calcine

Results of the various enthalpy-change measurements on samples of alumina coated with calcine are assembled in Table 18.

Gas was evolved from samples of this material in amounts which caused swelling of the platinum container-capsule at high temperatures. To avoid much swelling, most of the DC measurements were made at test temperatures about 750°C or below. The enthalpy change with the unirradiated specimens was measured only at T_h = 840° where the measured value was -3 cal/g.

As with the SEN-2 material, appreciable thermal effects were observed with unirradiated specimens in DSC measurements (see Figure 11). A small endothermic reaction ∿0.5 cal/g, started at about 60° and continued to 250°. Unlike SEN-2, a second endotherm of ∿2.5 cal/g occurred in the interval 480 to 600°C. The latter endotherm probably resulted from decomposition of metal nitrates or loss of chemically bound H_2O.

It is likely that several processes including gas evolution and stored radiation energy release from the alumina and calcine were contributing to the observed enthalpy changes. Our data are insufficient to separate the effects of the different processes. In any case, the net enthalpy change on heating irradiated specimens to 750°C or below appears to have reached approximate saturation of about 15 cal/g during the 6-week irradiation.

SEN-7, Hot Press

Results of the various enthalpy-change measurements on samples of this material are assembled in Table 19.

Gas was evolved from this material in amounts which caused swelling of the platinum container-capsule at high temperatures. To avoid much swelling with irradiated specimens, DC temperatures were held relatively low.

The SEN-7 material was formed by hot pressing (1000°C) at 50-50 mixture of quartz and PW-4m calcine (500°C).[30] The bonding between the hot pressed constituents was believed to result from the formation of small

amounts of Na_2O-SiO_2, which melts at about 780°, and Na_2-Fe_2O_3-SiO_2, which melts at about 760°C.[31] If these phases are, in fact, present, it is likely that melting of these contributed to the negative enthalpy change in unirradiated specimens upon heating to about 840°C Other effects caused the net release of 4.5 cal/g from unirradiated specimens in DSC measurements below 600°C (see Figure 15).

The major crystalline phases in the hot-pressed material prior to irradiation were quartz and components of PW-4m calcine.[30] It is known[28,29,33] that the effects of high-fluence neutron irradiation on quartz are similar to the effects on fused silica in the sense that the same vitreous phase is formed from each material. The density of this phase at high dose is greater than that of fused, vitreous silica by about 2.3%, and less than that of quartz by about 15%. Thermal annealing of the heavily irradiated materials apparently produces vitreous silica regardless of whether the initial material is quartz or fused silica. Accordingly, we assume that the enthalpy changes upon heating high-fluence specimens of quartz and fused silica are the same.

If we assume that the release of stored energy by the silica and the calcine in the irradiated samples of the hot-press material occurred independently of each other, we can estimate the contribution of silica to the observed values of ΔH, and thus find the contribution of the calcine and/or of interface materials and reactions. Using our data for the stored energy released fusion from irradiated silica (Table 6), our estimated values for the stored energy released from the silica in the high-fluence SEN-7 sample are $\sim$11 cal/g at 600°C and $\sim$30 cal/g at 800°C.

The observed release of stored energy from the high-fluence SEN-7 samples (Table 9) were $\sim$30 cal/g at 600 and 34 cal/g at 800°C. The net release after adjustment for observed thermal effects in unirradiated specimens of SEN-7 were $\sim$25 cal/g at 600°C and $\sim$38 cal/g at 800°C. Reducing the net values of stored radiation energy by the estimated contributions for

silica in the irradiated samples leaves 20 to 25 cal/g (40 to 50 cal/g of material other than silica) at both 600 and 800°C.* These amounts of energy must be ascribed to stored energy in the calcine and/or reactions between calcine and silica on heating the irradiated material, i.e., to reactions promoted by radiation damage in the material.**

SEN-4, Borosilicate Glasses

Results of the various enthalpy-change measurements on samples of this material are assembled in Table 20. Results of measurements of the average specific heat of irradiated and unirradiated samples are listed in Table 22.

The results of DSC measurements, Figure 13, showed no significant irreversible thermal effects upon heating to 600°. The indicated transformation temperature, T_g (transformation between a glass and a supercooled liquid) is between 495 and 500°C. The lack of irreversible thermal effects indicated that the enthalpy of the glass at a given temperature was not sensitive to the rate of cooling through T_g.†[34-36] Rapid relief of stresses in glasses takes place upon heating to and above T_g,[34] and it is likely that stored radiation energy also anneals rapidly upon heating to and above T_g. Assuming that this was the case, annealing of stored energy occurred rapidly at all the listed calorimeter temperatures at ~489°C and above.

The DC measurements on unirradiated specimens at T_h = 510°C showed an irreversible thermal effect in which 4 cal/g were evolved. Apparently changes occurred in the glass during the relatively long times (15-30 min) that a sample remained at 510°.[36] The nature of this change is unknown. The occurrence of changes during heating at 510° was also indicated by the

---

* Similar estimates for the low-fluence SEN-7 sample showed that the amounts of energy released which were not accounted for by the silica were also 20 to 25 cal/g.

** The indicated amounts of stored energy are much greater than found in either SEN-2 calcine samples (Table 17) or in SEN-1 samples of calcine on alumina Table 18. However, the radiation effects in the calcine may have been enhanced by the strains which must have resulted from the 15% swelling of the silica during irradiation. Also, the particular heat and pressure treatments used in the preparation of the SEN-7 material may have effected the susceptibility to radiation damage.

† The rate of cooling during manufacture of the glass was 1.5°C/min while that during the DSC measurement was about 20°C/min.

changes in the observed average heat capacity of both irradiated and unirradiated specimens after heating at 510° in the DC (Table 21). However, the information on specific heats is insufficient for evaluating the quantity $\Delta H(T_a) - \Delta H(T_i)$ [see Equation (13), Section 5.3]. The results of DC experiments in which the specimen was withdrawn from the calorimeter much more slowly than usual after the first drop showed no effects of withdrawal rate on ΔH and supported the idea that the enthalpy of the glass at a given temperature was not sensitive to the rates of cooling through T_g.

In principle, the DC values should be adjusted for the $\Delta H'(125)$ value of 4 cal/g and for possible differences between ΔH values at different annealing temperatures before comparing the DC and DSC stored energy results. (See Section 5.3.) However, as mentioned above, the information on specific heats is insufficient for evaluating possible differences between ΔH values at different temperatures. The agreement among the results in Table 20 suggests that any effects of an appreciable $\Delta H'(125)$ were cancelled by the effects of differences between effective annealing temperatures.

SEN-5, Borosilicate Glass

Results of the various enthalpy-change measurements on samples of this material are assembled in Table 21. Some results of measurements of the average specific heat of irradiated and unirradiated samples are listed in Table 22.

Generally, the discussions and interpretations given above for the SEN-4 glass samples apply also to this material and to the enthalpy-change results. The indicated transformation temperature T_g was between 508 and 512°C, about 12 degrees above that for SEN-4 (see Figure 14). It is likely that annealing of stored energy occurred rapidly at all the listed calorimeter temperatures above 500°C.

As with the SEN-4 samples, the DC measurements at 510°C on unannealed samples of SEN-5 showed an irreversible thermal effect. However, the $\Delta H'$-value for SEN-5 was 2 cal/g, one-half that of SEN-4.

As can be seen in Table 22, there is close agreement among all the ΔH values obtained at a given calorimeter temperature. There were no significant differences between the two different neutron exposures. The stored energy in these specimens, as indicated by both the DSC and DC results, was 20 cal/g.

Again, in principle, the DC values should be adjusted for the $\Delta H'(125)$ value (2 cal/g) and for possible differences between ΔH values at different effective annealing temperatures before comparing the DC and DSC stored energy results (see Section 5.3). However, as with the SEN-4 samples, the information on specific heats is insufficient for evaluations of possible difference between ΔH values at different temperatures. The agreement among the results in Table 22 suggests that any effects of an appreciable $\Delta H'(125)$ were cancelled by the effects of differences between effective annealing temperatures.

7.0 CONCLUSIONS

7.1 PREDICTED AMOUNTS OF STORED ENERGY AND AMOUNTS AND EFFECTS OF TEMPERATURE EXCURSIONS IN THE EVENT OF STORED ENERGY RELEASE

The main concerns with stored energy are: 1) that its rapid release may cause temperature rises which could be excessive with respect to the effects of high temperatures on the integrity of the waste-container and on the physical and chemical properties of the solid wastes, and 2) that the explosive release of mechanical energy accompanying a sudden temperature rise in the wastes might be of concern.

The results of this study show that large temperature excursions resulting from the release of the stored energy which may be accumulated during a period of ten years or more at relatively low storage temperatures following reprocessing are not possible. The temperature rises which could occur under adiabatic conditions and which represent the worst cases were estimated and are listed in Table 23 for the synthetic wastes included in this study. The values were calculated using the maximum observed stored energies and the measured heat capacities, assuming that a spontaneous release is triggered at 125°C and that the temperature rise occurs adiabatically. The maximum fast neutron doses to the calcines in SEN-1, -2, and -7 samples were equivalent to the damaging radiation doses which would accumulate within wastes during about 500 and 10 years following reprocessing for, respectively, LWR-UO_2 waste and mixed LWR-UO_2 (2/3) and LWR-PuO_2 (1/3) waste. The damaging doses to the glasses during neutron irradiations were much lower (Table 10) because the concentrations of fission product elements in the glasses were much lower; about 1/4 to 1/3 those in the calcines. However, the results obtained with the Cm-spiked glass samples (similar in composition to the SEN-4 samples) showed that damaging doses during 23°C storage exceeding those mentioned above for the calcines would not result in more than about 25 cal/g stored energy in the glass.

TABLE 23. Maximum Temperature Rises Resulting From Stored Energy Release

Specimen No. and Material	Maximum Observed and Fraction Observed ΔH, cal/g	Average Heat Capacity, cal/g/°C	Maximum Temperature Rise, °C
SEN-1 Calcine on Al_2O_3	15--all to 750°C	0.213	70
SEN-2 Calcine	25--all to >900°C	0.140	180
SEN-4 Glass	23.5--all	0.208	113
SEN-5 Glass	21-all	0.202	104
SEN-7 Hot Press	34--all to >800°C	0.219	155

No serious adverse effects on the waste container or on the physical and chemical properties of the wastes have been visualized as results of sudden temperature rises in the amounts shown in Table 23. Also, no serious mechanical effects are indicated. Thus, an instantaneous temperature rise of 250°C in 6.3 ft^3 of waste within a 12-in. ID canister would release a maximum of 1.7×10^5 cal of mechanical energy (assuming that the heat capacity and compressibility of the wastes are the same as those for Pyrex glass). The 1.7×10^5 cal represents an innocuous amount of mechanical energy. The linear expansion of the wastes resulting from the 250°C ΔT would be about 0.1%. The steel walls of the waste canister would easily accommodate the stress from this amount of expansion.

The results of this work also provide means of estimating the amounts of stored radiation energy (and accompanying hazards) which might accumulate during very long storage periods at the same relatively low, or at higher, storage temperatures.

The buildup of stored energy in the Cm-spiked borosilicate glass did not reach saturation at irradiation temperatures of 23°C and alpha doses of

up to 1.35×10^{18} α/g; corresponding to the total alpha decays during 1000 years storage after reprocessing of LWR-UO_2 wastes. However, the increase of stored energy with dose was very small following a dose of about 6×10^{17} α/g. Linear extrapolation of the experimental relationship between stored energy and dose in the dose range above 6×10^{17} α/g indicated about 35 cal/g at 10^6 years after reprocessing for the LWR-UO_2 wastes [$\sim$ 30,000 years for the mixed LWR-UO_2 (2/3) and LWR-PuO_2 (1/3) wastes]. Higher storage temperatures resulted in smaller amounts of stored energy in the Cm-spiked glass samples. These results indicate that the stored energy accumulation in borosilicate glass wastes will be less than $\sim$ 40 cal/g at the maximum. As discussed above, no serious adverse effects are expected to result from sudden release of this amount of stored energy.

Extrapolation of our experimental results for the calcine-containing specimens SEN-1, -2, and -7 are less clear-cut for several reasons including the facts that: 1) irreversible reactions with accompanying enthalpy changes which were unrelated to stored energy occurred upon heating, and 2) only two neutron doses were employed. However, from the results of the correlations of our experimental data and of other experimental data available in the literature, it was estimated that the saturation amounts of stored energy in these materials would be less than 50 cal/g.*

---

* The few data which are available on the effects of elevated temperatures during irradiation on the accumulation of radiation damage show that the amount of radiation damage at a given neutron dose generally decreases with increasing temperature.[4] However, in the particular case of alumina, it has been shown by Keilholtz and coworkers at ORNL that the radiation damage which is measured by swelling and crystal fracture increases with temperature in the range 100 to 600°C. This increase is associated with formation of clusters of defects. The stored energy associated with the clusters is unknown.[4]

  Radiation damage in the alumina in calcine-on-alumina type waste during storage would result primarily from alpha particle irradiation. We estimated that the number of atom displacements which occurred in our alumina samples during the 12-week neutron irradiations was about the same as the number which would occur during 10^6 years storage of calcines of mixed LWR-UO_2 (2/3) and LWR-PuO_2 (1/3) waste. Accordingly, even with some accelerating effects of elevated storage temperatures on the accumulation of stored energy, it is reasonable to assume that the maximum will not exceed about 50 cal/g (about twice that estimated for our 12-week neutron irradiated alumina samples).

7.2 COMPARISON OF THE EFFECTS OF ALPHA AND NEUTRON IRRADIATION

The observed amounts of stored energy with specimens of Melt 72-68 at high alpha doses and with SEN-4 (which had the same composition as the alpha-irradiated Melt 72-68 material) were in close agreement. The alpha-irradiated specimens contained 23.5 cal/g at the highest dose administered, and the neutron-irradiated specimens contained 21 to 23 cal/g. In both cases the stored energy was near saturation.

The stored energy appears to approach saturations at lower neutron doses than with alpha doses. The calculated neutron-recoil damage energies at the neutron fluences at which SEN-4 was irradiated are 1.4 and 3.6 x 10^{22} eV/g (see Sections 4.2 and 5.2.1.6). Alpha-RN damage energies equivalent to the neutron fluences are attained at 1.4 and 3.6 x 10^{17} α/g (assuming damage energy of 100 keV/α-RN). Comparison of the stored energy values observed at the two neutron fluences and with alpha irradiated specimens at equivalent doses is shown in Table 24. The apparent underestimate of the neutron damage energy is probably due in part to ignoring, in the calculations, the fission product element recoils with primary energies less than 0.025 MeV and the recoils of the low atomic weight elements.

TABLE 24. Comparison of Stored Energy[c] for Neutron and Alpha Irradiations at Equivalent Damage Energies[a]

Estimated Neutron Recoil Damage Energy, 10^{22} eV/g	Stored Energy cal/g	
	SEN-4 (Neutron Irradiated)	Melt 72-68[b] (Alpha Irradiated)
1.4	20.7	12.3
3.6	22.6	18.6

a. At 600°C annealing temperature.
b. Values taken from Figure 7. Conversion to equivalent neutron damage energy based on 100 KeV/-RN.
c. In cal/g.

8.0 REFERENCES

1. High-Level Waste Management Alternatives, Ed. K. J. Schneider and A. M. Platt, USAEC Report, BNWL-1900, vol. 1, May 1974.

2. M. J. Bell, ORIGEN-The ORNL Isotope Generation and Depletion Code, USAEC Report, ORNL-4628, May 1973.

3. High-Level Radioactive Waste Management Alternatives, USAEC Report, WASH-1297, May 1974.

4. G. H. Jenks and C. D. Bopp, "Energy Storage in High Level Radioactive Waste and Simulation and Measurement of Stored Energy with Synthetic Wastes," USAEC Report, ORNL-TM-3781, January 1973.

5. W. H. Huang and R. M. Walker, "Fossil Alpha-Particle Recoil Tracks: A New Method of Age Determination," Science, vol. 155, p. 1103, March 3, 1967.

6. M. T. Robinson and O. S. Oen, "Comments on "On the Atomic Displacement by Fast Neutrons' by Ohmae and Hida," J. Nucl. Mat., vol. 49, p. 101, 1973.

7. J. Linehard, V. Nielsen, M. Scharff and P. V. Thomsen, "Integral Equations Governing Radiation Effects," Mat. Fys. Nedd. Dan. Vid. Selsk. Vol. 33, no. 10, 1963.

8. G. H. Kinchin and R. S. Pease, "The Displacement of Atoms in Solids by Radiation," Rept. Progr. Phys., vol. 18, pp. 1-51, 1955.

9. J. O. Blomeke, C. W. Kee and J. P. Nichols, Projections of Radioactive Wastes to be Generated by the U. S. Nuclear Power Industry, ORNL-TM-3965, February 1974.

10. G. J. Dienes and G. H. Vineyard, Radiation Effects in Solids, Chapter 2, Interscience Publishers, New York, 1957.

11. D. F. Newman, "Radiation Damage in Borosilicate Glass," Quarterly Progress Report Research and Development Activities Waste Fixation Program, December 1972 through March 1973, BNWL-1741, pp. 30-38.

12. B. Domeij, F. Brown and M. McCargo, "Ranges of Heavy Ions in Amorphous Oxides," Can. J. of Phys., vol. 42, p. 1624, 1964.

13. H. D. Holland and D. Gottfried, "The Effect of Nuclear Radiation on the Structure of Zircon," Acta Cryst., vol. 8, pp. 291-300, 1955.

14. J. H. Crawford, Jr. and M. C. Wittels, "A Review of Investigations of Radiation Effects in Covalent and Ionic Crystals, Proceedings of the International Conference on Peaceful Uses of Atomic Energy, First Conference at Geneva, August 8-20, 1955, vol. 7 pp. 654-665, 1956.

15. N. E. Holden and F. W. Walker, "Chart of Nuclides, Knolls Atomic Power Lab., 11th Edition," revised to April 1972.

16. L. T. Lakey, et al., Development of Fluidized Bed Calcination of Aluminum Nitrate Wastes in the Wasted Calcining Facility, USAEC Report 100-14608, 1965.

17. E. J. Allen and H. T. Kerr, "Reevaluation of Neutron Fluxes for the ORR Stored Energy Experiments in the A-2 Position of the ORR Core," Letter to G. H. Jenks, January 6, 1975.

18. E. J. Allen and H. T. Kerr, "Neutron Flux Computational Model of the Oak Ridge Research Reactor," USAEC Report, ORNL-TM-4814, April 1975.

19. A. L. Boch, et al., "Radioactive Wastes Repository Project: Annual Progress Report for Period Ending September 30, 1972," USAEC Report, ORNL-4824, Oak Ridge National Laboratory pp. 201-8, December 1972.

20. Andre Roux, "Energie Emmagasinee dans les Oxydes BeO, MgO, Al_2O_3, et SiO_2 Irradies aux Neutrons," Thesis, University of Lyon, Report No. CEA-N-4171, translated by C. D. Bopp, December 1969.

21. Y. W. Touloukian, Ed., Thermodynamic Properties o High Temperature Materials, Macmillan Co., New York, vol. 4, pt. 1, p. 8, 1967.

22. Y. W. Touloukian, Ed., Thermodynamic Properties of High Temperature Materials, Macmillan Co., New York, vol. 4, pt. 2, p. 1655, 1967.

23. C. F. Lucks, H. W. Deem and W. D. Wood, "Thermal Properties of Six Glasses and Two Graphites," Am. Ceramic Soc. Bulletin, vol. 39, p. 313, 1960.

24. G. W. Morey, The Properties of Glass, Reinhold Publishing Corp., New York, p. 215, 1938.

25. B. S. Hickman and D. G. Walker, "The Effect of Neutron Irradiation on Aluminum Oxide," J. of Nucl. Materials, vol. 18, pp. 197-205, 1966.

26. M. Stevanovic and J. Elston, "Effect of Fast Neutron Irradiation in Sintered Alumina and Magnesia," Proc. Brit. Ceramic Soc., vol. 7, p. 423, 1967.

27. G. W. Keilholtz, R. E. Moore and H. E. Robertson, Effects of Fast Neutrons on Polycrystalline Alumina and Other Electrical Insulators at Temperatures from 60°C to 1230°C, USAEC Report, ORNL-4678, May 1971.

28. W. Primak and H. Szymanski, "Radiation Damage in Vitreous Silica: Annealing of the Density Changes," Phys. Rev., vol. 101, P. 1268, 1956.

29. William Primak, "Fast-Neutron Induced Changes in Quartz and Vitreous Silica," Phys. Rev., vol. 110, p. 1240, 1958.

30. G. J. McCarthy, "Crystalline Phase Formation in Calcined PW-6 and PW-4b," in Quarterly Progress Report Research and Development Activities Waste Fixation Program October-December 1973, BNWL-1809, pp. 63-65, January 1974.

31. G. J. McCarthy, "Quartz Isolation of Radioactive Wastes," J. of Materials Sci., vol. 8, pp. 1358-1359, 1973.

32. W. Primak, "A Review of the Gross Structural Effects of Energetic Atomic Particles on Vitreous and Crystalline Silica," J. Phys. Chem. Solids vol. 13, p. 279, 1960.

33. B. Lustman in Uranium Dioxide, Properties and Nuclear Application, Ed. J. Belle, p. 440, July 1961.

34. G. O. Jones, Glass, 2nd Ed., Chapman and Hall Ltd., 1971.

35. H. Scholze, "Reaction in Vitreous and Amorphous Solid," Reactivity of Solids, Eds., J. S. Anderson, F. W. Roberts and F. F. Stone, Chapman and Hall, London, Proceedings of the International Symposium on the Reactivity of Solids, Bristol, England, July 1972.

36. A. Q. Tool, "Effect of Heat Treatment on the Density and Constitution of High-Silica Glasses of the Borosilicate Type," J. Am. Ceramic Soc., vol. 31, p. 177, 1948.

DISTRIBUTION

No. of Copies

OFFSITE

UNITED STATES

A. A. Churm
ERDA Chicago Patent Group
9800 South Cass Avenue
Argonne, IL 60439

S. H. Smiley
Deputy Director for
Fuels and Materials
NRC Directorate of Licensing
for Fuels and Materials
4915 St. Elmo Ave.
Bethesda, MD 20014

R. B. Chitwood
Chief, Technical Support Branch
for Fuels and Materials
NRC Directorate of Licensing
for Fuels and Materials
4915 St. Elmo Ave.
Bethesda, MD 20014

W. P. Bishop
Chief, Waste Management Branch
NRC Division of Materials and
Fuel Cycle Facility Licensing
Washington, DC 20555

W. G. Belter
ERDA Division of Biomedical and
Environmental Research
Earth Sciences Branch
Washington, DC 20545

H. Glauberman
ERDA Division of Environmental
Control Technology
Washington, DC 20545

H. Hollister
ERDA Division of Environmental
Control Technology
Washington, DC 20545

No. of Copies

M. S. Kearney
ERDA Division of Environmental
Control Technology
Washington, DC 20545

W. E. Mott
ERDA Division of Environmental
Control Technology
Washington, DC 20545

F. P. Baranowski
ERDA Division of Nuclear Fuel
Cycle and Production
Washington, DC 20545

2 G. H. Daly
ERDA Division of Nuclear Fuel
Cycle and Production
Washington, DC 20545

O. P. Gormley
ERDA Division of Nuclear Fuel
Cycle and Production
Washington, DC 20545

A. F. Perge
ERDA Division of Nuclear Fuel
Cycle and Production
Washington, DC 20545

3 R. W. Ramsey
ERDA Division of Nuclear Fuel
Cycle and Production
Washington, DC 20545

E. E. Sinclair
Assistant Director for
Reactor Technology
ERDA Division of Reactor
Research and Development
Washington, DC 20545

W. H. McVey
Chief, Fuel Recycle Branch
ERDA Division of Reactor
Research and Development
Washington, DC 20545

No. of Copies

K. K. Kennedy
ERDA Idaho Operations Office
P. O. Box 2108
Idaho Falls, ID 83401

W. F. Hendrickson
ERDA Idaho Operations Office
P. O. Box 2108
Idaho Falls, ID 83401

E. H. Hardison
ERDA Oak Ridge Operations Office
P. O. Box X
Oak Ridge, TN 37830

O. T. Turmelle
ERDA Oak Ridge Operations Office
P. O. Box X
Oak Ridge, TN 37830

R. L. Chandler
ERDA Savannah River Operations Office
P. O. Box A
Aiken, SC 29801

C. D. Bopp
Oak Ridge National Laboratory
Oak Ridge Operations Office
P. O. Box X
Oak Ridge, TN 37830

30 G. H. Jenks
Oak Ridge National Laboratory
Oak Ridge Operations Office
P. O. Box X
Oak Ridge, TN 37830

200 ERDA Technical Information Center

J. A. Buckham
Allied Chemical Corporation
550 - 2nd Street
Idaho Falls, ID 83401

B. C. Musgrave
Allied Chemical Corporation
550 - 2nd Street
Idaho Falls, ID 83401

No. of Copies

C. M. Slansky
Allied Chemical Corporation
550 - 2nd Street
Idaho Falls, ID 83401

A. Schneider
Allied-Gulf Nuclear Services
P. O. Box 847
Barnwell, SC 29812

N. M. Levitz
Argonne National Laboratory
9700 South Cass Ave.
Argonne, IL 60439

M. J. Steindler/
L. E. Trevorrow
Argonne National Laboratory
9700 South Cass Ave.
Argonne, IL 60439

E. S. Bartlett
Battelle Memorial Institute
505 King Ave.
Columbus, OH 43201

J. J. Reilly
Brookhaven National Laboratory
Research Library,
Reference Section
Information Division
Upton, Long Island, NY 11973

R. H. Wiswall
Brookhaven National Laboratory
Research Library,
Reference Section
Information Division
Upton, Long Island, NY 11973

Chaim Braun
Brookhaven National Laboratory
Energy Systems Library
Building 902
Upton, NY 11973

Combustion Division
Combustion Engineering, Inc.
Windsor, CT 06095

No. of Copies

M. A. Thompson
Dow Chemical Company (ERDA)
Rocky Flats Division
P. O. Box 888
Golden, CO 80401

D. L. Ziegler
Dow Chemical Company (ERDA)
Rocky Flats Division
P. O. Box 888
Golden, CO 80401

C. H. Ice
duPont Company, Aiken (ERDA)
E. I. duPont DeNemours and Co.
Savannah River Laboratory
Aiken, SC 29801

A. S. Jennings
duPont Company, Aiken (ERDA)
E. I. duPont DeNemours and Co.
Savannah River Laboratory
Aiken, SC 29801

A. A. Johnson
duPont Company, Wilmington (ERDA)
E. I. duPont DeNemours and Co.
Wilmington, DE 19898

L. Henning
Electric Power Research Institute
3412 Hillview Ave.
P. O. Box 10412
Palo Alto, CA 94304

M. Levenson
Electric Power Research Institute
3412 Hillview Ave.
P. O. Box 10412
Palo Alto, CA 94304

E. Zebroski
Electric Power Research Institute
3412 Hillview Ave.
P. O. Box 10412
Palo Alto, CA 94304

No. of Copies

G. L. Meyer
Environmental Protection Agency
Technology Assessment Div. (AW-559)
Office of Radiation Programs
U. S. Environmental Protection Agency
Washington, DC 20460

B. Mann
Environmental Protection Agency
P. O. Box 15027
Las Vegas, NV 89114

R. E. Landreth
Environmental Protection Agency
5555 Ridge Ave.
Cincinnati, OH 45213

R. G. Barnes
General Electric Company
175 Curtner Ave.
(M/C 160)
San Jose, CA 95125

E. E. Voiland
General Electric Company
Midwest Fuel Recovery Plant
Route 1, Box 219-B
Morris, IL 60450

W. H. Reas
General Electric Company
Vallecitos Nuclear Center
Vallecitos Road
Pleasanton, CA 94566

L. H. Brooks
Gulf Energy and Environmental Systems
P. O. Box 81608
San Diego, CA 92138

Central Research Library
Document Reference Section
Holifield National Laboratory (ERDA)
Oak Ridge, TN 37830

No. of Copies

Central Research Library, ORNL
Holifield National Laboratory (ERDA)
Oak Ridge, TN 37830

Laboratory Records Dept., ORNL
Holifield National Laboratory (ERDA)
Oak Ridge, TN 37830

Laboratory Records Dept., ORNL-RC
Holifield National Laboratory (ERDA)
Oak Ridge, TN 37830

C. W. Christenson
Los Alamos Scientific Laboratory (ERDA)
P. O. Box 1663
Los Alamos, NM 87544

L. J. Johnson
Los Alamos Scientific Laboratory (ERDA)
P. O. Box 1663
Los Alamos, NM 87544

H. S. Jordan
Los Alamos Scientific Laboratory (ERDA)
P. O. Box 1663
Los Alamos, NM 87544

C. J. Kershner
Monsanto Research Corporation Mound Laboratory
P. O. Box 32
Miamisburg, OH 45342

P. Lamberger
Monsanto Research Corporation Mound Laboratory
P. O. Box 32
Miamisburg, OH 45342

Stephen Brown
National Lead Company
111 Broadway
New York, NY 10006

No. of Copies

D. Cyrus Klingsberg
Technical Secretary
National Academy of Sciences
Committee of Radioactive Waste Management
National Research Council
2101 Constitution Avenue
Washington, DC 20418

T. Lash
Natural Resources Defense Council, Inc.
664 Hamilton Avenue
Palo Alto, CA 94301

J. P. Duckworth,
Plant Manager
Nuclear Fuel Services, Inc.
P. O. Box 124
West Valley, NY 14171

E. D. North, Director of Technical Administration
Nuclear Fuel Services, Inc.
6000 Executive Blvd., Suite 600
Rockville, MD 20852

W. L. Pearl
Nuclear Water and Waste Technology, Inc.
P. O. Box 6406
San Jose, CA 95150

J. G. Cline, General Manager
NYS Atomic and Space Development Authority
230 Park Avenue, Rm. 2425
New York, NY 10017

Frank von Hippel
Princeton University Center for Environmental Studies, Engineering School
Princeton, NJ 08540

W. Weart
Sandia Laboratories
Albuquerque, NM 87107

No. of Copies

J. Sivinski
Sandia Laboratories
Albuquerque, NM 87107

B. R. Teer
Transnuclear, Inc.
One North Broadway
White Plains, NY 10601

J. O. Blomeke
Union Carbide Corporation (HNL)
Chemical Technology Division
P. O. Box Y
Oak Ridge, TN 37830

D. E. Ferguson
Union Carbide Corporation (HNL)
Chemical Technology Division
P. O. Box Y
Oak Ridge, TN 37830

E. H. Kobisk
Union Carbide Corporation (HNL)
Chemical Technology Division
P. O. Box Y
Oak Ridge, TN 37830

K. H. Lin
Union Carbide Corporation (HNL)
Chemical Technology Division
P. O. Box Y
Oak Ridge, TN 37830

W. C. McClain
Union Carbide Corporation (HNL)
Chemical Technology Division
P. O. Box Y
Oak Ridge, TN 37830

W. C. Ulrich
Union Carbide Corporation (HNL)
Chemical Technology Division
P. O. Box Y
Oak Ridge, TN 37830

S. E. Logan
University of New Mexico
Albuquerque, NM 87131

No. of Copies

R. A. Beall
U.S. Department of Interior
Bureau of Mines
Albany Research Center
1450 W. Queen Avenue
Albany, OR 97321

FOREIGN

Rene Amavis
EURATOM
Health Physics Division
29, Rue Aldringer
Luxembourg, BELGIUM

K. D. B. Johnson
Atomic Energy Research Establishment
Harwell, Didcot,
Berks, ENGLAND

D. W. Clelland
United Kingdom Atomic Energy Authority
Risley, ENGLAND

R. Bonniaud
Centre de Marcoule
B. P. 106
30 - Bagnols S/Ceze
FRANCE

P. J. Regnaut
Centre d'Etudes Nucleaires de Fontenay-aux-Roses
Boite Postale 6
92 - Fontenay-aux-Roses
FRANCE

J. Sauteron
Centre d'Etudes Nucleaires de Fontenay-aux-Roses
Boite Postale 6
92 - Fontenay-aux-Roses
FRANCE

No. of Copies

Y. J. Sousselier
Centre d'Etudes Nucleaires
de Fontenay-aux-Roses
Boite Postale 6
92 - Fontenay-aux-Roses
FRANCE

E. R. Merz
Institut für Chemische
Technologie
Kernforschungsanloge
Julich GmbH
D517 Julich
Postfach 365
GERMANY

K. H. Rattay
Institut für Chemische
Technologie
Kernforschungsanloge
Julich GmbH
D517 Julich
Postfach 365
GERMANY

W. Heimerl
Institut für Chemische
Technologie
Kernforschunsanloge
Julich GmbH
D517 Julich
Postfach 1913
GERMANY

W. A. Issel
KEWA Kernbrennstoff-
Wiederaufarbeitungs-
Gesellschuft m.b.H.
Projecktleitung
7501 Leopoldshafen
Postfach 60
GERMANY

H. Krause
Nuclear Research Center
Waste Management Dept.
D75 Karlsruhe
Weberstr. 5
GERMANY

No. of Copies

H. Witte
NUKEM GmbH
645 Hanau 11
Postfach 110080
WEST GERMANY

Giacomo Calleri
CNEN
Directorate di Programma
Eurex Del CNEN
Saluggia "Vercelli", ITALY

Willy Bocola
CNEN
Laboratorio di Ingegneria
Sanitaria
Via Anguillarese km 1 + 300
Roma, ITALY

Ferruccio Gera
Laboratorio Rifiuti Radioattivi
C.N.E.N. - C.S.N. Casaccia
Casella Postale 2400
00100 Rome, ITALY

N. S. Sunder Rajan
Bhabha Atomic Research Centre
Waste Treatment Division
Trombay, Bombay, INDIA

K. T. Thomas
Bhabha Atomic Research Centre
Waste Treatment Division
Trombay, Bombay, INDIA

R. V. Amalraj
C.W.M.F. Project
P. O. Kalpakkam
Chingleput Dist.
Tamil Nadu, INDIA

2 International Atomic Energy
Agency
Kärtner Ring 11
P. O. Box 590
A-1011, Vienna, AUSTRIA

No. of Copies

H. F. Randohr
c/o Friedrich Uhde GmbH
46 Durtmund
Deggingstr. 10-12
GERMANY

ONSITE

6 ERDA Richland Operations Office

O. J. Elgert
R. B. Goranson
N. T. Karagianes
R. D. Fogerson
D. J. Squires
F. R. Standerfer

7 Atlantic Richfield Hanford Company

D. R. Gustafson
R. E. Isaacson
D. C. Nelson
A. E. Smith/M. J. Szulinski
J. H. Warren
D. D. Wodrich
File Copy

1 Exxon
Richland, WA 99352

S. J. Beard

1 Joint Center for Graduate Study

J. Cooper

3 United Nuclear Industries, Inc.

A. P. Larrick

2 Westinghouse Hanford Company

A. G. Blasewitz
C. R. Cooley

lbe

No. of Copies

67 Battelle-Northwest

T. W. Ambrose
J. W. Bartlett
R. J. Bashor
C. L. Brown
L. L. Burger
H. C. Burkholder
N. E. Carter
M. O. Cloninger
G. J. Dau
R. L. Dillon
J. R. Eliason
J. W. Finnigan
J. C. Fox
J. J. Fuquay
B. Griggs
J. H. Jarrett
R. S. Kemper
M. R. Kreiter
K. M. Harmon
R. C. Liikala
J. L. McElroy
L. K. Mudge
R. G. Nelson
R. E. Nightingale
D. E. Olesen
A. M. Platt
J. A. Powell
F. P. Roberts (25)
K. J. Schneider
P. C. Walkup
E. J. Wheelwright
L. D. Williams
W. K. Winegardner
H. H. Van Tuyl
Technical Information (5)
Technical Publications (3)